Dynamic of organic matter and meiofaunal community on a river-dominated shelf (Rhône prodelta, NW Mediterranean Sea): responses to river regime

A.M. Pruski, Jadwiga Rzeznik-Orignac, Philippe Kerhervé, Gilles Vétion, Solveig Bourgeois, Erwan Peru, Pablo Brosset, Flora Toussaint, Christophe Rabouille

HAL Id: hal-03178286

https://hal.sorbonne-universite.fr/hal-03178286

Submitted on 23 Mar 2021

1   Dynamic of organic matter and meiofaunal community on a river-dominated shelf

2   (Rhône prodelta, NW Mediterranean Sea): responses to river regime

3

4

5

6   Author names and affiliation

7   Audrey M. Pruski[a], Jadwiga Rzeznik-Orignac[a], Philippe Kerhervé[b], Gilles Vétion[a], Solveig Bourgeois[a], Erwan

8   Peru[a], Pablo Brosset[a], Flora Toussaint[c], Christophe Rabouille[c]

9

10   [a] Sorbonne Université, CNRS, Laboratoire d'Ecogéochimie des Environnements Benthiques, LECOB, F-

11   66650 Banyuls-sur-Mer, France

12   [b] Université de Perpignan Via Domitia, CNRS, Centre de Formation et de Recherche sur les

13   Environnements Méditerranéens, CEFREM, F-66860 Perpignan, France

14   [c] Laboratoire des Sciences du Climat et de l'Environnement, LSCE/IPSL,CEA-CNRS-UVSQ-Université Paris

15   Saclay, 91198 Gif-sur-Yvette, France

16

17   Corresponding author : Audrey M. Pruski, 1 avenue Pierre Fabre, Observatoire Océanologique de

18   Banyuls, 66650 Banyuls sur mer, France

19   Email : audrey.pruski@obs-banyuls.fr

20   Tel : 00 33 4 68 88 73 79

21   Abstract:

22   In the oligotrophic context of the Mediterranean Sea, riverine inputs of particulate organic matter

23   represent an important source of food for benthic communities. However, since most of these inputs

24   are delivered during short, but intense flood events, communities living in the vicinity of river mouths

25   are also exposed to strong and frequent physical disturbances. A very tight and complex relationship

26   links river dynamic and macrofaunal communities in Mediterranean deltas, but less is known on the

27   response of meiobenthic communities to river regime. In 2010, sediments cores were collected in the

28   Rhône River prodelta in winter and spring before the flooding of the Rhône River tributaries in June, and

29   then twice in the early and late summer. The hypothesis was that increased runoff and export of

30   terrigenous material would induce major changes in the sediment biochemistry, which would in turn

31   trigger modifications in abundances and vertical distribution of the meiofauna. The origin and quality

32   (lability, degradation state) of the different pools of organic matter preserved in these recent sediments

33   were determined using bulk geochemical and molecular analyses (fatty acids, amino acids). Vertical

34   profiles of descriptors for organic matter origin and quality revealed major changes in the nature of the

35   inputs occurring at monthly time scales. Inputs of plant detritus from autumnal and winter flood events

36   were still visible in the cores collected in February and April. A few days after the June 2010 high-

37   discharge event, a newly deposit (~ 7 cm) containing soil organic matter has recovered the prodeltaic

38   sediments and the resident meiofaunal community, but at the end of August only 2 cm of this deposit

39   remained. Multivariate analyses furthermore highlighted that the meiofaunal community was driven by

40   both the trophic conditions and deposition of a new sediment layer driven by the hydrological regime

41   of the Rhône River. In April, increased abundances of meiofauna were observed in response to the

42   sedimentation of labile organic matter after the spring bloom. The June high-discharge event affected

43   the meiofauna with a reduction of its abundance and the burial of the resident meiobenthic community.

44   However, the meiofauna recovered in less than two months after this disturbance, showing the strong

45   resilience of this component of the benthic ecosystem in this high energy environment.

1. Introduction

Rivers represent the main source of fresh water, nutrients, sediments and terrestrial organic carbon (OC) to the coastal ocean. Continental shelves influenced by large to medium-sized rivers consequently account for some of the most biologically productive marine systems on Earth and have great ecological, biogeochemical, social and economic values (Day et al., 2019b). River flow dynamic, land use, coastal circulation, resuspension and meteorological events are all parameters that exert some level of control on the delivery and dispersal of riverine inputs of sediments and OC on the shelf. Human activities such as deforestation, agriculture, urbanisation, fluvial regulation and diversion affect the land-ocean export, both quantitatively and qualitatively (Bianchi and Allison, 2009). These transitional areas are also particularly vulnerable to climate-driven disturbances associated with global warming, sea-level rise and the increasing frequency and intensity of storms (O'Leary et al., 2017). How natural and anthropogenic changes in the delivery of terrestrial OC to continental shelves will affect global OC budgets remains largely uncertain (Bauer et al., 2013). Likewise, benthic communities play a central role in the cycling and burial of OC in estuarine ecosystems, but they are particularly exposed to combined anthropogenic stressors (Akoumianaki et al., 2013, 2006; Martin et al., 2019). Given this, the question is how and to what extent, changes in river inputs have an impact on benthic communities and the regulating services they provide.

Deltas are peculiar estuaries that form where sand and mud supply exceeds sediment dispersal. Their existence and functioning are therefore closely linked to river inputs (Giosan et al., 2014). A plethora of river delta systems have formed in the microtidal wave-influenced setting of the Mediterranean Sea (Besset et al., 2017). The watersheds and fluvial regime of most Mediterranean deltas, including the Ebro, Rhône, Po and Nile, have undergone severe modifications to accommodate human activities (Day et al., 2019a). Despite considerable efforts to control the runoff of these rivers, the export of particulate matter takes place primarily during high discharge flood events triggered by intense rainfalls or oceanic storms (Antonelli et al., 2008). Depending on the season and drainage basin affected, the magnitude and nature of the particulate organic matter (POM) exported during these

74 events are highly variable with inputs of fossil OC, eroded soils, riparian vegetation or phytoplankton

75 (Antonelli et al., 2008; Cathalot et al., 2013; Harmelin-Vivien et al., 2010; Higueras et al., 2014; Marion

76 et al., 2010; Tesi et al., 2008). Meteorological and hydrological drivers are thus expected to control the

77 supply and quality of the POM delivered to the shelf as well as its bioavailability for the benthic fauna.

78 Moreover, extreme flooding events results in the rapid deposition of fine terrigenous particles which

79 have significant effects on the structure and function of macrobenthic communities (Cardoso et al.,

80 2008; Lohrer et al., 2004; Norkko et al., 2002). For instance, off the Rhône River, the proliferation of

81 opportunist species taking advantage of flood deposits has been observed in the months following

82 major events (Salen-Picard et al., 2003). A very tight and complex relationship links river dynamic and

83 macrofaunal communities in Mediterranean deltas (Akoumianaki and Nicolaidou, 2007; Bonifácio et al.,

84 2014; Hermand et al., 2008; Salen-Picard et al., 2003). By contrast, meiobenthic communities (animals

85 retained between 40 µm and 1 mm mesh size of sieves; Giere, 2009) from deltaic systems have received

86 little attention (Danovaro et al., 2000; Guidi-Guilvard and Buscail, 1995; Palacín et al., 1992, Semprucci

87 et al., 2019) at the notable exception of foraminiferans (Fontanier et al., 2008; Franzo et al., 2019;

88 Goineau et al., 2012). The meiofauna has an important role in the functioning of benthic ecosystem,

89 contributes significantly to the diet of many other animals (Coull, 1990), and facilitates mineralisation

90 of organic material (Coull, 1999; Gee, 1989; Riera and Hubas, 2003). Because of their small size, lack of

91 larval stage and shorter generation time, meiobenthic organisms respond more successfully than the

92 macrofauna to changes in environmental conditions (Balsamo et al., 2012). As such, meiofaunal

93 communities have been widely used to monitor the effects of both natural and anthropogenic

94 perturbations in aquatic ecosystems (Coull and Chandler, 1992; Gambi et al., 2003; Schratzberger and

95 Ingels, 2018, Semprucci et al., 2018). Although the meiofauna appears as a good bioindicator of organic

96 enrichment and physical disturbance in coastal areas (Gambi et al., 2003), there is a paucity of studies

97 focusing on their response to river inputs (Danovaro et al., 2000; Guidi-Guilvard and Buscail, 1995;

98 Palacín et al., 1992; Pelletier et al., 1999).

99   In this study, the response of meiofaunal communities to the dynamic of river inputs is

100   discussed. In 2010, we had the opportunity to study the impact of a high-discharge event of the Rhône

101   River, the largest Mediterranean river. Sediments were collected in the winter and spring before this

102   period and afterwards, twice in the early and late summer. The hypothesis was that this extreme event

103   would induce major changes in the sediment biochemistry, which would in turn trigger modifications in

104   abundances and vertical distribution of the meiofauna. The specific aims of the present study were (1)

105   to evaluate how the Rhône River regime affect sediment biochemistry in the prodelta at a seasonal time

106   scale, (2) to investigate whether the main taxa of the meiofauna respond to changes in river inputs, and

107   (3) to determine which of the investigated environmental parameters (i.e. grain-size, porosity,

108   sedimentary organic matter composition, stable isotopic values…) were the most pertinent to illustrate

109   the observed trends. A particular attention was paid at determining the origins and quality of the POM

110   delivered by the Rhône River, as it represents fresh sources of detritus for benthic organisms.

111

112   2. Materials and methods

113   2.1. Regional setting and study area

114   The Rhône River, now the main river in the Mediterranean Sea since the damming of the Nile,

115   links the Rhône glacier in the Swiss upper Alps to the Camargue delta on the French coast of the

116   Mediterranean Sea (the Gulf of Lion). It is mainly an Alpine river, which drains a relatively small (95,000

117   km^2), but highly diversified, watershed exhibiting a strong geological heterogeneity (Olivier et al., 2009).

118   The Rhône catchment includes several climatic zones (mountainous, oceanic and Mediterranean)

119   resulting in a very complex hydrological regime and a strong inter annual variability (Pont et al., 2002).

120   Typical of Mediterranean rivers, the runoff of the Rhône is characterised by flooding events triggered

121   by intense rainfalls in autumn and snowmelt in spring. As a consequence, solid export to the Gulf of Lion

122   occurs mainly during short, but intense high-discharge events (Antonelli et al., 2008). Riverine

123   particulate inputs undergo a rapid deposition near the river mouth in the prograding prodelta (Maillet

124   et al., 2006). The unconsolidated sediments are frequently resuspended by episodes of strong winds or

125   by near bottom currents (Ulses et al., 2008). The study area is located at 2.5 km of the Rhône River

126   mouth in the prodelta area (Fig. 1).
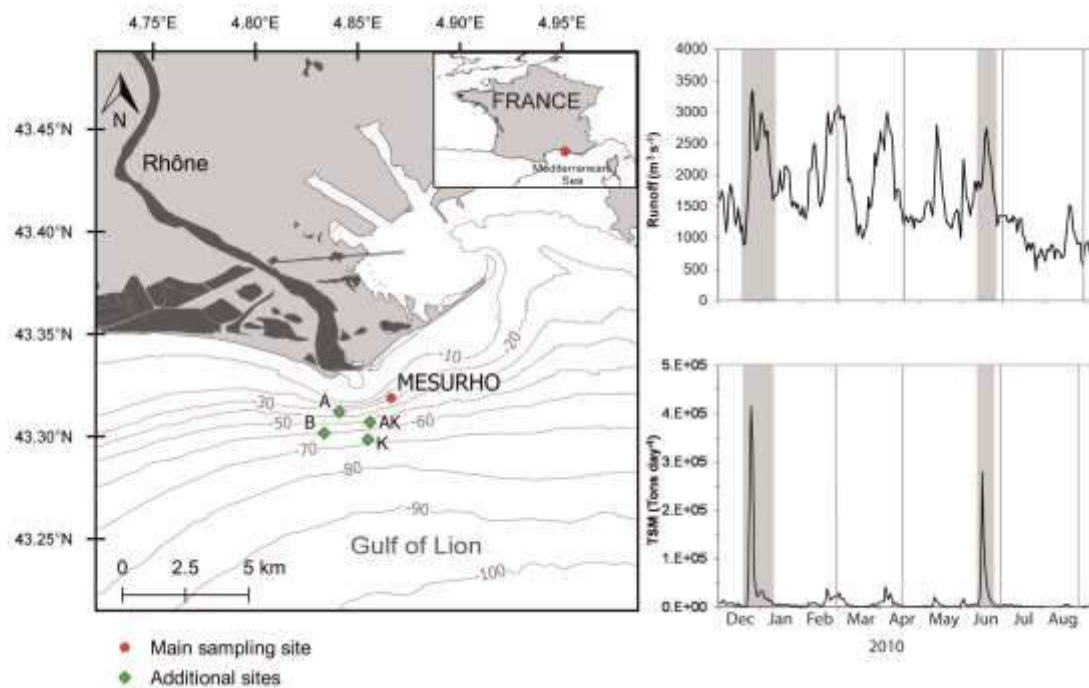
127

128   **Figure 1: Location of the sampling sites in the Gulf of Lion (left) and Rhône River runoff and total**
129   **suspended matter (TSM) concentration for 2010 (right).** Rhône data were measured at the SORA
130   Observatory Station in Arles, the most downstream gauge station, 40 km upstream the mouth. The
131   vertical bars indicate the sampling dates and the grey areas represent periods of high solid discharge
132   rate.

133

134   2.2. Hydrological and climatic conditions

135   Mean daily discharge data from the Arles gauging station were provided by the CNR (Compagnie

136   Nationale du Rhône, the main hydropower company on the Rhône River). Daily total suspended matter

137   (TSM) concentrations measured in water samples collected at the Rhône observatory station at Arles

138   (SORA) were provided by the MOOSE network (Mediterranean Oceanic Observing System for the

139   Environment – http://www.moose-network.fr). Monthly weather reports were provided by Météo

140   France.

141

142

143   2.3. Sediment sampling

144   The sampling targeted four contrasted periods in 2010: winter (20th February), spring (18th

145   April), early (1st July) and late summer (28th August). Sediment cores were collected at station MESURHO

146   (43°19.2 N, 4°52 E, 20 m depth) from the board of the Téthys II R/V using a multicorer MUC 8/100

147   (Oktopus GmbH) during the field campaigns MESURHOBENT 1, 2, 3 and 4 (Rabouille, 2010a, b, c, d). At

148   each sampling date, four undisturbed sediment cores (9.5 cm of diameter and 60 cm of height) were

149   processed on board and sliced into seven horizontal layers (0–0.5, 0.5–1, 1–2, 2–3, 3–5, 5–7 and 7–10

150   cm). Since previous studies in the prodelta area have shown that variability among cores was low

151   (Bourgeois et al., 2011; Cathalot et al., 2010; Pastor et al., 2011a), one core was conditioned in this study

152   for sediment characterisation. Sediment layers were carefully homogenised, distributed in two aliquots

153   and immediately frozen at -20°C. Sediment layers from the three other cores were preserved in 70%

154   alcohol for meiofaunal analysis. Visual observation of the sediment cores used in this study showed no

155   signs of burrows, biogenic structures, oxic voids or large macrofauna, suggesting low bioturbation

156   activity.

157

158   2.4. Assessment of sediment characteristics

159   Sediment granulometry was assessed using a Malvern® Mastersizer 2000 laser diffraction

160   particle size analyser. Porosity (φ) was calculated by determining water mass loss during drying

161   assuming a value of 2.63 g.cm^{-3} for grain size density and 1.03 g.cm^{-3} for pore water density. Sediment

162   granulometry, and porosity were determined in triplicate for each sample.

163   Elemental and biochemical analyses were performed on freeze-dried sediments. The analytic

164   protocols for total organic carbon (TOC), bulk stable carbon isotopes (δ^{13}C), total hydrolysable amino

165   acids (THAA) and fatty acids have been described in Fagervold et al. (2014).

166   Enzymatically hydrolysable amino acids (EHAA), which correspond to the fraction of amino acids

167   assumed to be bioavailable for benthic deposit-feeders, were extracted by the biomimetic approach of

168   Mayer et al. (1995). THAAs and EHAAs were analysed by reverse phase high-performance liquid

169 chromatography (HPLC, Gynkotek-Dionex system) following precolumn derivatisation with

170 orthophtaldialdehyde (Lindroth and Mopper, 1979). The isoindol derivatives were separated on a C18-

171 HPLC column using a non-linear gradient of methanol-acetate buffer and were detected by fluorescence

172 at 450 nm using an excitation wavelength of 335 nm (Bourgeois et al., 2011).

173 Fatty acid, THAA and EHAA concentrations were normalised to total organic carbon.

174

175 2.5. Assessment of meiofaunal abundance and taxonomic composition

176 The sediment samples were sieved through 1000 and 40 µm mesh simultaneously. The fraction

177 retained on the 40 µm sieve was collected and centrifuged with Ludox HS 40 (density 1.15) as described

178 by Heip et al. (1985). The organisms in the supernatant were collected and rinsed on a 40 µm mesh to

179 remove Ludox and preserved in 70% alcohol. All meiobenthic organisms were counted and classified to

180 higher taxon under a stereomicroscope, after staining with rose Bengal. A sample splitter, Motoda-box

181 (Motoda, 1959) was used to obtain an aliquot containing about 1000 organisms, for the abundance

182 estimations of nematodes and copepods. The number of other meiobenthic taxa was too low to

183 evaluate on split samples, they were thus counted on the whole sample. Total density of meiofauna and

184 of the main representative taxa (nematodes, copepods, annelids, cumaceans, turbellarians,

185 foraminiferans, and kinorhynchs) were determined (number of individuals/10 cm^2) for the four sampling

186 dates. Mean density based on the 3 cores were calculated for each layer. Note that the Ludox extraction

187 is less efficient for organisms with shells, like foraminiferans, molluscs or ostracods, and that the

188 abundances were thus underestimated for these taxa.

189

190 2.6. In situ microprofiling of dissolved oxygen and DOU calculation

191 A benthic lander carrying a benthic microprofiler (Unisense®) was deployed to measure *in situ*

192 microprofiles of dissolved oxygen (Cai and Reimers, 1993; Rabouille et al., 2003; Rassmann et al., 2020

193 and references therein). The benthic lander was deployed in April, July and August 2010 at a maximum

194 of 5 stations, except in August because of bad weather conditions. These stations encompass the

195   MESURHO station, another proximal station located in the South of the Rhône River (A), and 3 other

196   stations located in the Rhône prodelta (AK, B and K, Fig. 1).

197   Four oxygen microelectrodes were simultaneously deployed, and vertical depth profiles were

198   measured with a 200 µm resolution together with a resistivity electrode. As their response to variations

199   in oxygen concentrations is linear (Boudreau and Jorgensen, 2001), the O_2 microelectrodes were

200   calibrated with a two-point calibration technique using the bottom water O_2 concentration determined

201   by Winkler titration and the anoxic pore waters. Signal drift of O_2 microelectrodes during profiling was

202   checked to be less than 5 %. Diffusive oxygen uptake (DOU) rates were calculated using Fick's first law

203   (Berner, 1980, Eq. 3),

204
$$DOU = -\emptyset \cdot D_s \cdot \frac{d[O_2]}{dz}\bigg|_{z=0} \qquad (3)$$

205   where ϕ is sediment porosity, Ds the diffusion coefficient in the sediments ($cm^2\ s^{-1}$), and

206    $\frac{d[O_2]}{dz}\big|_{z=0}$ is the oxygen gradient below the sediment water interface ($\mu mol\ cm^{-4}$). For the calculations,

207   the gradient between 0 and 400 µm in the sediment was consistently used. The Ds coefficients were

208   adjusted for diffusion in a porous environment according to: $D_s = \frac{D_0}{(1+3\cdot(1-\emptyset))}$ with the diffusion

209   coefficient in free water (D_0) taken from Broecker and Peng (1974) and recalculated at *in situ*

210   temperature using Li and Gregory (1974).

211

212   2.7. Data analysis

213   The amount, sources, and quality of the sedimentary organic matter (OM) in the Rhône prodelta

214   were assessed with a suite of bulk and molecular descriptors. The list of the parameters used in this

215   study is provided in Table 1 with their interpretation. The degradation index (DI) was calculated from

216   the molar composition of the THAA hydrolysates (Dauwe et al., 1999a). This index synthesises subtle

217   changes in the amino acid composition linked with diagenesis into a univariate variable indicative of OM

218   degradation stage, whose value decreases with increasing degradation. We applied the same calculation

219   on the EHAA composition of the flood deposit. In this case, the index (DI_{EHAA}) provided information on

220 the degradation stage of the pool of amino acids that may be assimilated by benthic organisms. The

221 reactivity index [RI=(tyrosine+phenylalanine)/(β-alanine+ɣbutyric acid)] is another indicator of OM

222 degradation (Jennerjahn and Ittekkot, 1997). It takes into account two opposite trends: the reactive

223 aromatic amino acids, tyrosine and phenylalanine, are rapidly degraded in decaying OM, whereas their

224 decarboxylation products, β-alanine and ɣ-butyric acid, consistently increase with microbial degradation

225 (Alkhatib et al., 2012; Jennerjahn and Ittekkot, 1997).

226 A one-way ANOVA was used to analyse variations in total meiofaunal abundance whereas two-

227 ways ANOVA were performed to test for differences in meiofaunal vertical distribution with time, with

228 sediment depth and time x sediment depth. Abundances were double square root transformed in order

229 to meet the assumptions for ANOVA (homogeneity of variances, normally distributed residuals). A Tukey

230 Honest Significance Test (HSD) test was applied when significant differences were detected between

231 means. Analyses of variance were run with XLSTAT (V4.01).

232 A principal component analysis (PCA) was then performed to reveal trends in OM composition

233 that could help us retrace the recent history of riverine particle inputs in the prodelta. Prior to PCA, a

234 correlation analysis of the environmental variables was performed to identify variables that were highly

235 correlated, retaining only one of these variables. PCA was combined to hierarchical clustering of the

236 PCA components (HCPC), which determines clusters of samples that present homogenous

237 characteristics (Husson et al., 2010). The HCPC was performed on the 5 first components of the PCA

238 (accounting for 91% of the total variance) using Ward's agglomerative method and a Euclidean distance.

239 PCA and HCPC were performed using R software (3.4.4) with the package 'Rcmdr – Factominer' (Lê et

240 al., 2008).

241 Relationships between the abundance of meiofaunal taxa and factors, representing sediment

242 characteristics, were summarised using a Canonical Correspondence Analysis (CCA) (ter Braak, 1986)

243 performed with the R package 'vegan' (Oksanen et al., 2016). CCA allowed to simultaneously visualise

244 the abundances of the principal meiofaunal taxa, the optimal niches (sample corresponding to sediment

245 depth × date) with the environmental parameters (Borcard et al., 2011). The environmental variables

246 identified by PCA were first retained. The "vif.cca" function of 'vegan' was then used to identify

247 redundant constraints (i.e. environmental variables with variance inflation factors >10) and were

248 removed from the analysis to reduce collinearity. CCA was finally performed on square root transformed

249 abundances to reduce the weight of abundant taxa and a subset of standardised environmental

250 variables describing the quality of food available for the meiofauna ($\delta^{13}C$, C/N ratio, normalised

251 concentration in EHAA, EHAA/THAA ratio, DI, % Algal PUFA) or related to sediment properties (porosity,

252 % clay, and $CaCO_3$). The statistical significance of the overall relationship and of the canonical axes were

253 evaluated using Monte Carlo permutation tests (999 permutations). The CCA ordination diagram

254 displayed samples and taxa as points and environmental variables as vectors (Borcard et al., 2011).

255 Finally, the relative importance of the explanatory variables was evaluated by forward selection

256 followed by Monte Carlo permutation tests (999 permutations) using the "ordistep" function of 'vegan'

257 (Blanchet et al., 2008). With this method, all variables are ranked on the basis of their marginal effects

258 (i.e. considering each variable as the sole constraining variable) and conditional effects (i.e. forward

259 selection on the best descriptors and evaluation of the fit of each variable in conjunction with the

260 variable(s) already selected).

261 Result outputs for ANOVA and multivariate analyses are provided in the supplementary

262 material.

263

264 **3. Results and discussion**

265 **3.1. Hydrological and climatological conditions**

266 In 2010, the French Mediterranean coast experienced a cold and rainy winter with strong winds

267 dominated by Mistral. Rains were frequent, but moderate with Rhône water discharge reaching 2500m^3

268 s^{-1} ten days before February sampling and 3000m^3 s^{-1} on the sampling date (Fig. 1). The organic content

269 of the total suspended matter (TSM) was high (TOC= 7.81% on the 12th of February 2010, Kerhervé

270 unpublished result). March was also rainy and windy. Two minor floods occurred before the April

271 sampling, but TSM only slightly increased during these events. In April, the weather was fair with little

272 wind and precipitation, but liquid discharge rates were high, possibly because of snow melting. As a

273 consequence, TSM increased above 100mg.L^{-1}. On the 15th and 16th of June 2010, exceptional stormy

274 rains (40cm per day) have generated severe flooding in south-eastern France. This rare and deadly flash

275 flood event is believed to be the most important since 1827 (Payrastre et al., 2012). Rainfalls mostly

276 affected the southeast tributaries of the Rhône River (the Durance, the Buëch, the Verdon, etc.) causing

277 their overflow. The runoff of the Rhône River peaked at 2600m^3.s^{-1}, while solid discharge reached 2.8

278 10^5 tones on June 16, 2010. In the days before return to normal runoff, the Rhône brought

279 approximately one fourth of the annual solid input for 2010. The summer was dry and hot. The daily

280 runoff rate was below the mean inter annual flow rate of 1700 m^{3}s^{-1} and was typical of low river flow

281 (500-1000 m^{3}s^{-1}). July was characterised by strong winds generally oriented N-NW (12 to 13 days of

282 Mistral). The wind changed of direction on the 26th of July (S) and generated a storm regime.

283 Meteorological conditions were similar on August with episodes of strong winds.

284

285 **3.2 Oxygen penetration depth and metabolic activity traced by diffusive oxygen uptake (DOU) in the**

286 **Rhône prodelta**

287 The oxygen microprofiles recorded *in situ* at station MESURHO display a large decrease below

288 the sediment-water interface over depth of a few millimetres, below which the sediment was

289 completely anoxic (Fig. 2). A clear change in time for the oxygen penetration depth (OPD) is visible on

290 figure 2 with average values of 1.4 ± 0.5 mm in April 2010, 2.6 ± 0.5 mm in July 2010, and 2.4 ± 0.2 mm

291 in August 2010.

April 2010   July 2010   August 2010
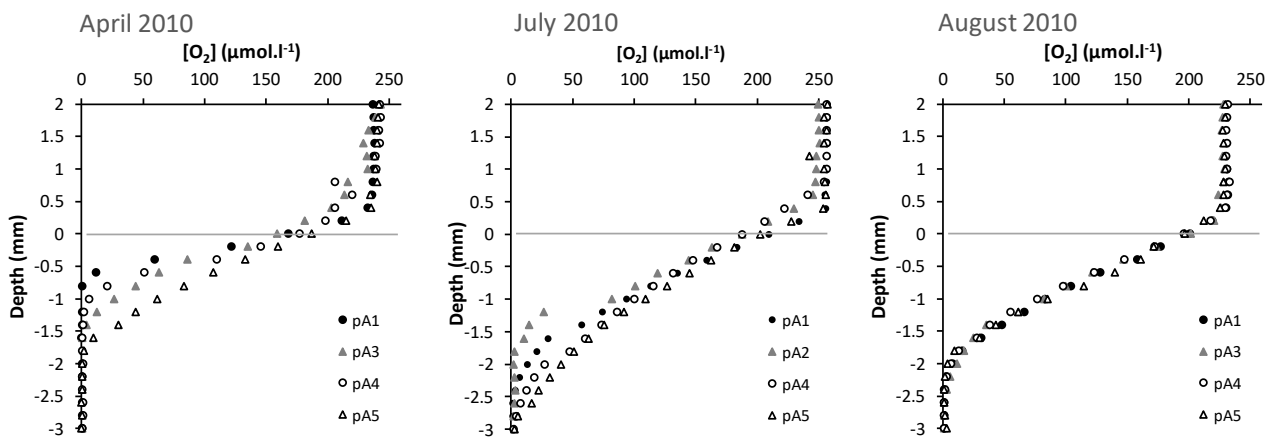
Figure 2: Dissolved oxygen microprofiles at the sediment-water interface recorded *in situ* at the MESURHO station in April, July, and August 2010. Each symbol represents a single electrode profile. The line at 0 mm indicates the sediment surface.

This increase in OPD is accompanied by a decrease of DOU (Table 2), which is a proxy of the metabolic activity in the sediments based on organic matter mineralisation (Cathalot et al., 2010; Rassmann et al., 2020). The DOU recorded at 5 stations in the prodelta show a decrease from April to July, with a levelling in August for the only record that we have at the MESURHO station. The decrease of DOU at the spring-summer transition in 2010 contrasts with the normal spring-summer situation with fresh organic matter deposition and bottom water warming, which generates more mineralisation in surface sediments (Lansard et al., 2008). This unusual decrease in early summer could be related to the high-discharge event in June and the deposition on the seabed of low reactivity material as happened in 2008 during a flood carrying significant amount of material from the Durance tributary (Cathalot et al., 2010). The decrease was more pronounced for stations MESURHO and AK (~ 40% decrease), which are directly under the influence of the Rhône River inputs, and more limited for stations B and K, suggesting lower disturbance with increasing distance from the river mouth.

310 **3.3. Short-term chronicle of particulate organic matter inputs in the Rhône prodelta**

311   Short sediment cores collected in deltaic areas are useful records of the recent history of

312 riverine POM inputs in coastal areas (Cathalot et al., 2010; Leithold and Hope, 1999). The down-core

313 evolution of sedimentary OM composition provides insights on temporal changes in the characteristics

314 of the POM available for the benthic fauna (Goineau et al., 2012). Clearly, the down-core profiles of

315 organic compounds are far from a textbook situation with steady inputs of OM from the overlying water

316 and progressive degradation on the seafloor (see for instance TOC profiles, Fig. 3). Likewise, descriptors

317 of OM origin (δ^{13}C, fatty acid subgroups) and quality (C/N, EHAA/THAA, DI, RI) point to major changes in

318 the nature of the inputs occurring at a monthly time scale (Fig. 3).

319   In February, sampling occurred early at the very onset of a Rhône River flood. High organic

320 contents were observed through the sedimentary column, with an integrated TOC content of 1.4% for

321 the ten first centimetres of sediment (Fig. 3). The normalised concentrations in THAA and fatty acids

322 were also high. Descriptors of OM quality and origins revealed strong differences between the surface

323 sediment and the layers below. Phytoplankton markers were only found in the upper layer indicating

324 either the rapid degradation of this labile fraction within the sediments or a recent pulse of POM

325 deriving from microalgae. This assumption is further supported by an enriched δ^{13}C value as well as by

326 descriptors of OM quality (DI, RI, and EHAA/THAA ratio), which exhibited slightly higher values on the

327 surface than in the layers below (Fig. 3). Subsurface and deeper layers were enriched in coarse material

328 and markers of plant detritus (long chain fatty acids) and had a constant C/N ratio of ~10. These

329 biomarkers associated to high TOC contents and a coarser material are consistent with the preservation

330 of plant detritus brought in autumn and winter.
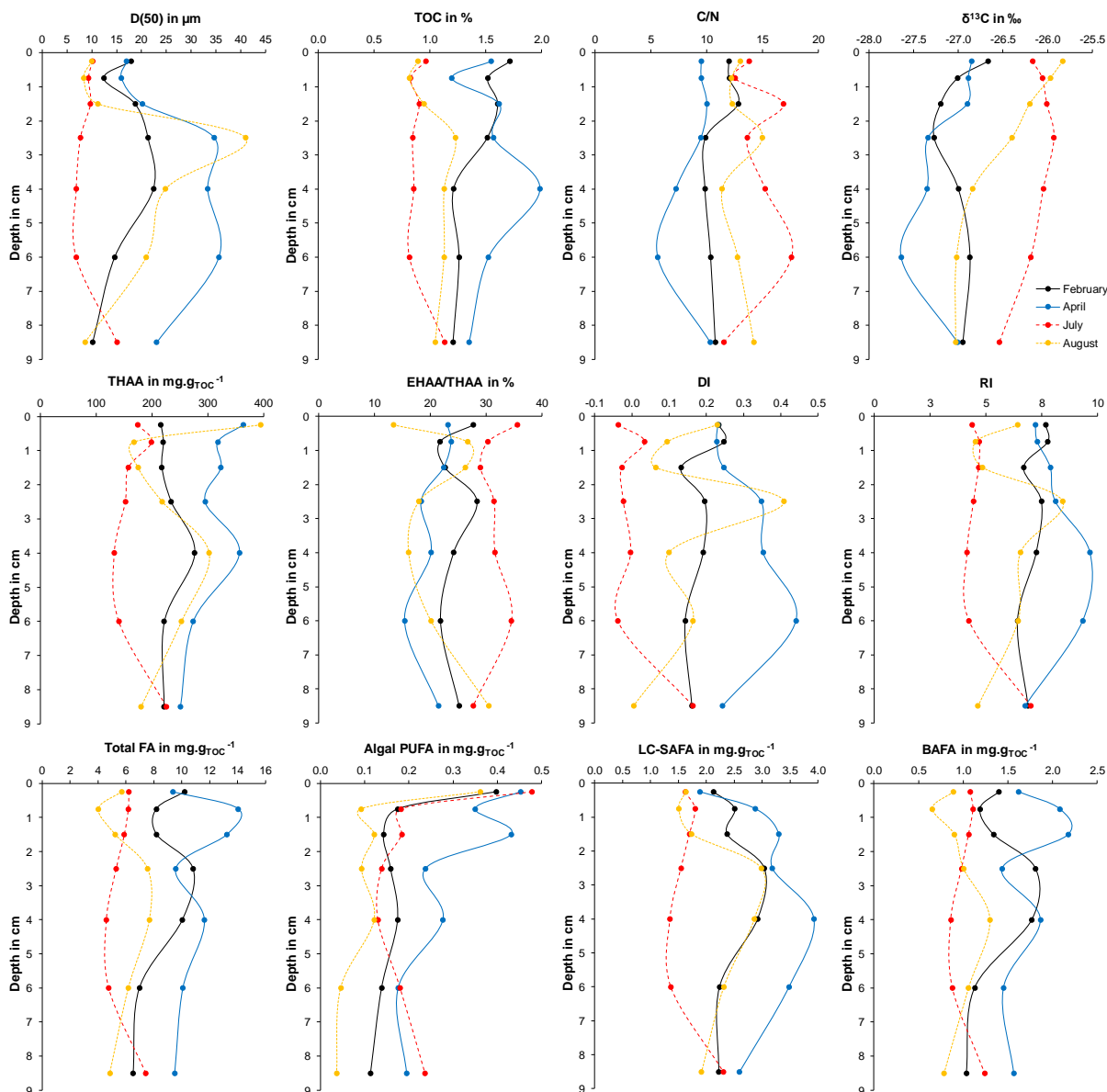
Figure 3: Down-core evolutions of sediment properties at the MESURHO station in February, April, July, and August 2010. D(50)= median grain size, TOC= total organic carbon, C/N= molecular carbon to nitrogen ratio, $\delta^{13}C$= bulk stable isotope value, THAA= normalised total hydrolysable amino acid concentration, EHAA/THAA= proportion of enzymatically hydrolysable amino acids, DI= degradation index value, RI= reactivity index, Total FA, Algal PUFA, LC-SAFA and BAFA= TOC-normalised concentrations in total fatty acids, algal polyunsaturated fatty acids, long chain saturated fatty acids and bacterial fatty acids.

In April, sedimentary characteristics were more heterogeneous on the 10cm layer than during the winter (Fig. 3). TOC content was still high and comparable to February in the surface sediment, but

342 at 3-7cm depth, a layer enriched in markers of plant detritus was observed. At the surface, high

343 concentrations in planktonic markers were again suggestive of phytoplankton inputs. Organic carbon,

344 amino acids and fatty acids tended to be higher in the subsurface sediments. This coarser subsurface

345 layer was also less degraded (higher DI and RI) with a lower bioavailability of the amino acid pool.

346 Globally, this suite of descriptors indicates that plant detritus have been exported during the two floods

347 that preceded the sampling, or that earlier deposits in the mud belt have been remobilised. Porosity

348 was also discontinuous, in agreement with the successive deposition of different layers of material.

349   The grain size distribution shows the deposition of about 7 cm of fine particles on the sediment

350 after the torrential rainfalls in June (Fig. 3, 96% of particles <63µm). The sudden peak of TSM (Fig. 1)

351 certainly accounted for this deposit, which was depleted in organic carbon and nitrogen. The flood

352 deposit was also depleted in labile components such as fatty acids and hydrolysable amino acids (on

353 average only ~7% of the TOC was found in the THAA) and was globally more degraded (lower DI and RI)

354 than the material delivered during periods of normal discharge. The characteristics of this fine material

355 recall the one delivered by the Rhône River during the flood of the Durance tributary in June 2008

356 (Bonifácio et al., 2014; Pastor et al., 2018). Following this event, a flood deposit of ~30 cm was observed

357 in the prodelta area (Cathalot et al., 2010). This organic-poor material had a peculiar δ^{13}C signature (-

358 25.8‰) and displayed a Δ^{14}C of -495‰ in relation with the refractory nature of the eroded watershed

359 and the flushing of the Serre-Ponçon dam on the Durance (Cathalot et al., 2013; Copard et al., 2018).

360 The decrease in remineralisation activity in the surface sediments after these two events is a further

361 indication that the deposited material was poorly reactive (Table 2).

362   The trend for lower porosities at the end of August suggests that the summer conditions allowed

363 the muddy deposits to settle and become more compact (Table S1, supplementary material). This is

364 consistent with the concomitant stratification of the microbial community described by Fagervold et al.

365 (2014) at this station. Organic content was still low, but OM characteristics indicate intense reworking

366 of the sediments since July (Fig. 3). δ^{13}C values ranged from "flood signature" of the tributaries (~ -26‰)

367 in surface to the usual winter value of the Rhône (~ -27‰). Below the first two centimetres, which kept

368   the flood imprint, the sediment was enriched in TOC, amino acids, fatty acids, and long chain fatty acids.

369   The down-core evolution of the DI is difficult to interpret. In the surface layer (0-0.5cm), the DI value

370   was similar to values found in February and April on the top of the cores and may be indicative of the

371   recent export of TSM by the Rhône River. Values for the 0.5-1 and 1-2cm layers were closed to those

372   found in the flood deposit, between 2-3cm depth DI was similar to values measured in the April layer

373   enriched with macrodetritus, and below DI was lower indicative of a more degraded pool of POM. Grain

374   size followed the same trend as DI in good consistency with the hypothesis that the 2-3cm layer

375   corresponded to sediments enriched in coarse macrodetritus. The proportion of bioavailable amino

376   acids (EHAA/THAA) was also extremely variable along the sediment depth consistent with inputs of

377   different sources of POM and non-steady state conditions.

378   Taken together all these results show that the flood deposit formed a thinner layer at the end

379   of the summer in comparison to what settled in June. Estimation of the thickness of this layer is about

380   1.5 to 2 cm depending on the parameters used. Compaction cannot entirely account for the reduction

381   of the thickness of the flood deposit. Erosion is the most likely explanation. Strong winds occurred in

382   July (26th) causing the resuspension of sediments at the MESURHO buoy (Lorthiois, 2012). The author

383   described the sediment dynamic during this event as the resuspension of the non-consolidated

384   sediments and their near bottom transport offshore. Dufois et al. (2014) have demonstrated that

385   bottom erosion could be an important process for the sediment dynamic in the prodelta area during

386   moderate river discharge and energetic events. Above the remaining flood deposit, some inputs of fresh

387   suspended particulate matter (DI= 0.23) enriched in labile biogenic compounds (amino acids and fatty

388   acids) have settled during the summer (Fig. 3). Underneath the flood deposit, older consolidated

389   deposits from the autumn, winter and/or spring were found.

390

391

392

393 ### 3.4. Sources and lability of the sedimentary organic matter in the Rhône prodelta

394   Down-core evolutions of bulk and molecular descriptors of sedimentary organics in the prodelta

395 highlight the occurrence of several pools of OM, whose dynamic of delivery is related to season and

396 river regime. A PCA was performed to define the biochemical properties of these different pools of OM

397 (Fig. 4).
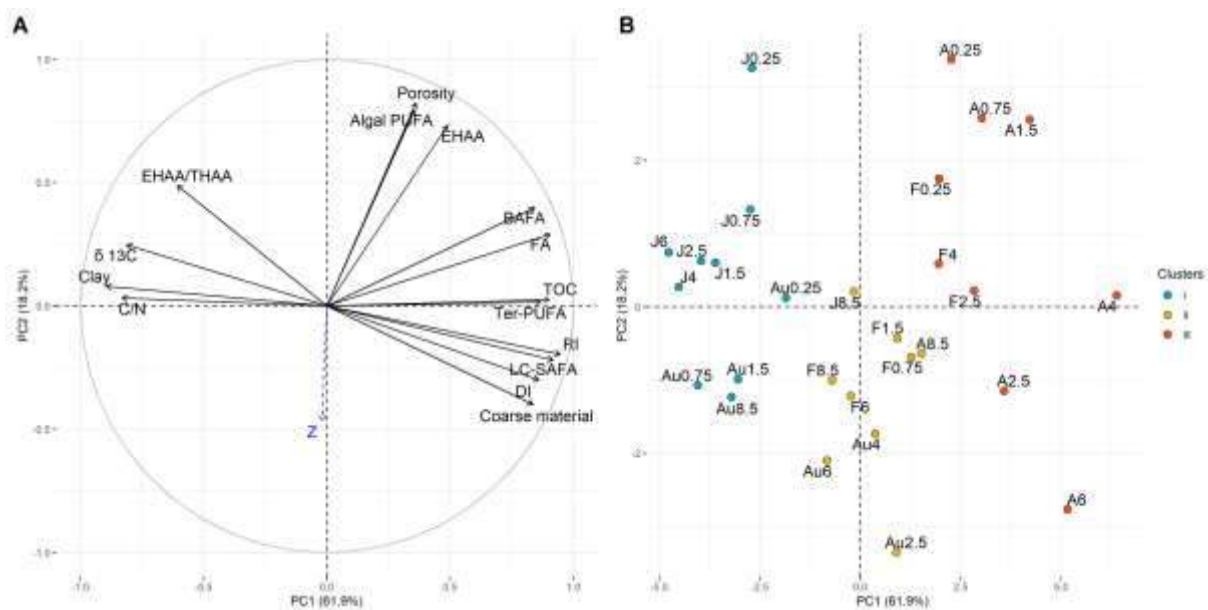
398

399 Figure 4: Principal component analysis (PCA) of sediments collected in the Rhône River prodelta: loading

400 plot (A) and score plot (B) for the first and second principal components (7 sediment layers × 4 dates).

401 Black arrows indicate active variables and the blue arrow corresponds to the supplementary variable

402 (sediment depth: Z). Samples were clustered in 3 groups according to a hierarchical clustering analysis

403 performed on the 5 first principal components of the PCA. Sample code is as follow: the letter indicates

404 the month (F= February, A= April, J= July, Au= August) and the number corresponds to the mid-depth

405 of the sediment layer (in cm). Clay= % of particles <4μm, Coarse material= % of particles >200μm, $CaCO_3$

406 = % of calcium carbonate. For all other variables see Table 1 for abbreviations. Concentrations in EHAA,

407 fatty acids (FA), BAFA, LC-SAFA, Terrestrial PUFA & Algal PUFA were normalised to organic carbon

408 content.

409

410   Results of the PCA show that sediment properties can be summarised in two independent

411 principal components explaining 80% of the total variance (Fig. 4A). Sediment layers were not grouped

412 by dates or strata on the two first components of the PCA (Fig. 4B), which is consistent with the

413 successive deposition of particles originating from different sources. Two pools of organic inputs were

414 clearly separated on the first component axis (PC1= 61.9 % of the total variance). A group of variables

415 with positive loadings on PC1 characterised a coarser material enriched in TOC, fatty acids, and markers

416 of vascular plants (LC-SAFA and Ter PUFA). This material also exhibited higher DI and RI values, indicative

417 of limited diagenetic alteration, and depleted δ^{13}C values consistent with an input of modern plant

418 detritus in C3 (δ^{13}C plant = -28‰, Hedges et al., 1986). Taken together, these results confirm that

419 sediment cores collected in February and April 2010 were enriched in plant detritus (Fig. 4B, cluster II).

420 A distinct source of OM associated to clay, low TOC content, higher C/N ratios and δ^{13}C values was found

421 in June and some sediment layers in August 2010 (negative loadings on PC1 and cluster I). OM in the

422 flood deposit (Cluster I) was also more bioavailable for the benthic fauna as seen by higher EHAA/THAA

423 ratios (Fig. 3). The second principal component (PC2= 18.2% of the total variance) illustrates variations

424 that can be attributed to sediment depth, such as the decrease in porosity in the sedimentary column

425 and the rapid degradation of the most labile components (PUFA deriving from phytoplankton and

426 EHAA). The distribution of layers from the April core along PC2 agrees with this general pattern: the 2

427 first centimetres (with positive loadings) being enriched in bioavailable OM, whereas the layers below

428 (with negative loadings) contained a more refractory pool of OM. A second group of samples

429 characterised by lower algal contents and porosity was also linked to PC2. This cluster regroups

430 intermediate layers from August and some layers from February (cluster II on Fig. 4B).

431 The different molecular descriptors used in this study enable to explore the relationships

432 between two fundamental properties of the OM, its origin and its quality. A positive relationship

433 between DI and EHAA/THAA ratio has been previously evidenced supporting the idea that as OM is

434 degraded in the sediments, it becomes less available to enzymes (Dauwe et al., 1999b). Here, the

435 reverse relationship was observed with a significant negative correlation between DI and EHAA/THAA

436 ratio. The mixing of different pools of terrestrial OM may explain these opposite results. A study focusing

437 on the benthic food web in a Mediterranean lagoon has revealed that different types of plants displayed

438 contrasted levels of bioavailability with terrestrial plants exhibiting low EHAA/THAA ratios (10.4-18.1%),

439   seagrasses having intermediary values (12.2-33.4%), and salt marsh vegetation representing a highly

440   digestive source of OM (50.0-60.2%) (Carlier et al., 2007). In good agreement with these earlier results,

441   macrodetritus isolated from sediments at the MESURHO station have a low digestibility (EHAA/THAA

442   ratio = 9.8) and a DI value (0.29) in the range of those calculated for the layers enriched in plant detritus

443   (Pruski, unpublished result). As a general trend bioavailability was thus higher when the contribution of

444   plant detritus was lower (r^2=0.85). Consequently, the lower bioavailability observed in February, April

445   and some layers from August may be attributed to the presence of macrodetritus. There was also a

446   positive correlation between the DI and the proportion of fatty acids specific of epicuticular waxes from

447   leaves (LC-SAFA) indicating that macrodetritus represent in our system a source of fresh OM, and that

448   LC-SAFA are good tracers of litter inputs (i.e. they are less abundant in soils than in the litter).

449   In the flood deposit, soils certainly account for most of the particulate OC exported to the

450   prodelta as observed previously after the flood of June 2008 (Cathalot et al., 2013). This hypothesis is

451   supported by low contributions of biomarkers of phytoplankton and higher plant detritus. The different

452   indexes of degradation provide contrasted insights on the history of this material. The low values of the

453   amino acid based degradation indexes (DI and RI) indicate that the POC exported during the June flood

454   was more degraded than the material delivered during periods of normal river regime (Bourgeois et al.,

455   2011). This is consistent with the weathering of degraded POM from soils or riparian areas during

456   intense rainfall events and the decrease of benthic microbial remineralisation (lower DOU in July and

457   August, Table 2). However, the flood deposit was also characterised by high EHAA/THAA ratios (on

458   average 32% in the flood deposit versus 23% in the February and April cores). The higher bioavailability

459   of this material is somewhat counterintuitive. One would expect soil OM to be less prone to enzymatic

460   digestion than fresh detritus. From this point of view, the particulate matter transferred to the sea

461   during the 2008 and 2010 high-discharge events differed remarkably (EHAA/THAA ~20% in 2008,

462   Bonifácio et al., 2014). In 2008, strong rainfalls were responsible for the opening of the spillway of the

463   Serre Ponçon dam (Marion et al., 2010). Silts were eroded from black marls of the Durance watershed.

464   As a consequence, this material was old and refractory (Δ^{14}C= -495.1‰ ± 1.7 in Cathalot et al., 2013;

465   DI= -0.13, Bourgeois unpublished result). Differences in bioavailability between the TSM delivered

466   during the 2008 and 2010 events may be related to the watersheds affected by the precipitation and

467   the nature of the material transported. Low pigment concentrations in the material exported in June

468   2010 (Fagervold et al., 2014) indicate that EHAA were mostly associated to non-algal OM, and certainly

469   incorporated to geopolymers as humic substances (Burdige and Martens, 1988). The exported SPM

470   furthermore contained two pools of OM with distinct amino acid compositions: the first and dominant

471   pool was more degraded than the OM delivered during periods of normal discharge (negative DI of the

472   THAAs -0.02±0.03), while another minor fraction of the OM was more labile as shown by elevated DI

473   values calculated on the EHAA (DI_{EHAA} ~0.33± 0.01 for the flood deposit).

474

475   ### 3.5. Temporal changes in meiofaunal community

476   Meiofaunal abundances increased from February (2137 ± 1401 ind. 10 cm^{-2}) to April (9818 ±

477   2027 ind. 10 cm^{-2}) with intermediate abundances in July (6025 ± 1375 ind. 10 cm^{-2}) and August (4574 ±

478   1394 ind. 10 cm^{-2}) (Fig. 5). Nematodes were the most abundant metazoans (70%), followed by

479   harpacticoid copepods (18 %), annelids (4.5%), kinorhynchs (4%), foraminiferans (2%), cumaceans (1%)

480   and turbellarians (0.5%) (Supplementary material, Table S2). This community structure was typical of

481   soft bottom habitats (Danovaro et al., 2000; Giere, 2009; Moodley et al., 2000).

482   Total abundances of meiofauna (Fig. 5) were in the same range as those reported for other sites

483   in the Gulf of Lion (de Bovée et al., 1990; Grémare et al., 2002). Differences between dates were

484   statistically significant (one-way ANOVA, F=15.75, p < 0.001). Pairwise comparisons revealed

485   significantly higher abundances in April and significantly lower in February (Tukey post hoc test,

486   Supplementary material, Tables S3 and S4). The fivefold increase in the meiofaunal abundance from

487   February to April coincided with the inputs of fresh and labile OM on the sea floor (enrichment in algal

488   PUFA and amino acids, Fig. 3). Peaks of abundance are frequently observed after the post-bloom

489   sedimentation of phytodetritus (Palacín et al., 1992; Vanaverbeke et al., 2004). Giere (2009) reported

490   that decaying phytoplankton results in the deposition of a fluffy layer of phytodetritus on the sediment

491   and, after a short time (a few days), those unconsolidated organic deposits enhance the bacterial activity

492   and cause a significant increase in meiofaunal abundance.
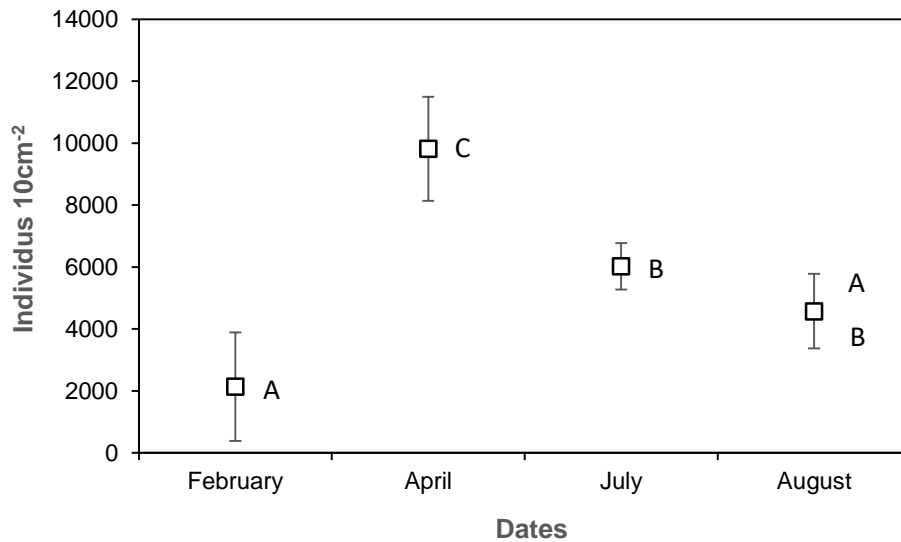

493

494   **Figure 5: Total meiofaunal abundances at the MESURHO station in February, April, July, and August 2010.**

495   Values are means ± SD (n = 3 cores). Analysis of variance (one-way ANOVA, F=15.75, p < 0.001) and

496   Tukey post hoc test, dates sharing the same letters are not significantly different.

497

498   Results from the two-way ANOVA show the significant effect of sediment depth on the

499   distribution of the meiofauna (F=26.87, p < 0.001). Significant "date x sediment depth" interaction terms

500   (F=3.95; p < 0.001) furthermore indicate that the vertical distribution of the meiofauna differed

501   between sampling periods (Table S5). In February, April and August, the vertical distribution of the

502   meiofauna showed a typical pattern with high abundances near the surface (0-3 cm depth) and

503   decreasing abundances with sediment depth (Fig. 6) as already described by Soetaert et al. (1995) and

504   Vanreusel et al. (1995). The highest values were recorded on the first 2 cm of the cores, which

505   corresponded to the layers of sediment enriched in phytodetritus (Fig. 3). This vertical pattern could be

506   due to the active migration of the meiofauna to the food source accumulated on the sediment surface

507   (Franco et al., 2008; Moens et al., 2013). Sediment oxygenation could be another regulating factor since

oxygen penetration in the sediment was very limited in the prodelta area (Fig. 2). Oxic niches were thus

509 only available close to the sediment–water interface.

510
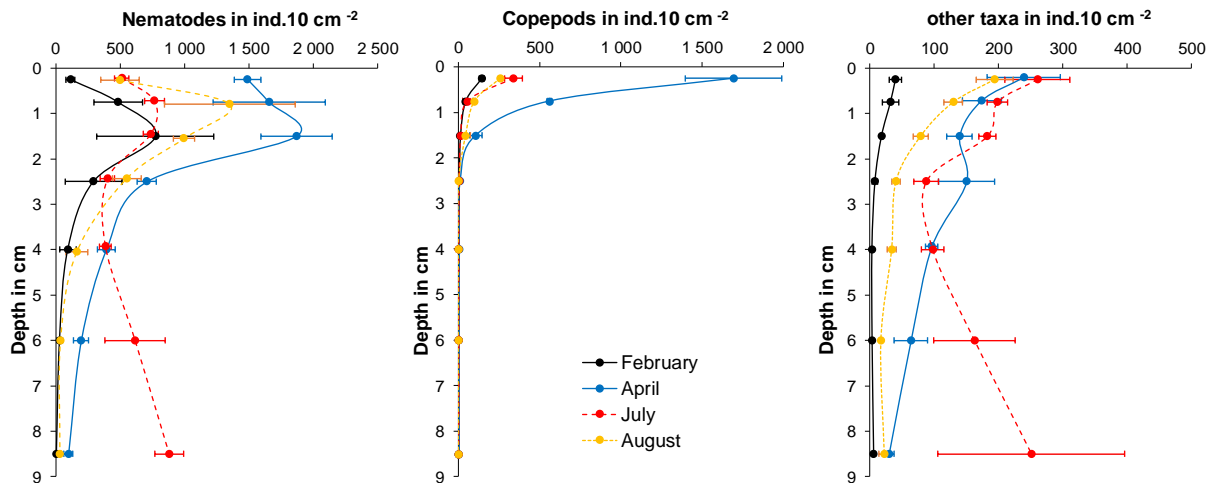
Figure 6: Vertical distribution of meiofauna (nematodes, copepods and other taxa) at the MESURHO station in February, April, July and August 2010. Values are means ± SEM (n=3 cores). Note that some symbols were slightly shifted vertically relative to each other for visibility.

515

516   The vertical distribution of the meiofauna in July differed from the general pattern with high

517 abundances in the deep layers similar to those recorded in the very upper layers of the other dates

518 (two-way ANOVA, $p < 0.001$, Supplementary material, Table S5). The vertical profiles of copepods seem

519 to fit the pattern of oxygen penetration depth (Fig. 2), but this clearly does not apply to nematodes and

520 foraminiferans, which displayed the highest abundances in deep sediment layers (5 to 10 cm depth,

521 Supplementary material, Table S2). These changes in the vertical distribution of the main meiofaunal

522 taxa occurred just a couple of days after the flood of the Rhône tributaries and the sudden increase in

523 TSM (Fig. 1). The drop in meiofaunal total abundance and the presence of a high density of nematodes

524 in the deep layers after this high-discharge event can be explained by the burial of the meiobenthic

525 community as observed experimentally with the simulated deposition of dredged material

526 (Schratzberger et al., 2004). As so the present results corroborate the observation of Pelletier (1999)

527 that high-discharge events severely affect the meiofauna with a reduction of its abundance. Among the

528 "other taxa" the clear dominance of foraminifera from genus *Leptohalysis* was noted in July. This

529 foraminiferan is considered as an opportunistic taxon resistant to high turbidity, large inputs of

530 terrestrially-derived OM, and low oxygen penetration in the sediment (Mojtahid et al., 2009; Scott et

531 al., 2005). An opportunistic strategy allows *Leptohalysis* to proliferate in the Rhône prodelta in just a

532 few days after a flood (Goineau et al., 2012).

533 In August, the community had already recovered a pre-disturbance structure. This short

534 resilience time may be explained by a particularity of the study site. The Gulf of Lion is a highly

535 hydrodynamic system, exposed to frequent strong winds and weather conditions where the benthic

536 ecosystem undergoes frequent physical disturbance (Pont et al., 2002). High hydrodynamism can

537 promote meiofaunal recolonisation. Indeed, while strong currents mechanically remove meiofauna

538 from sediment, the first phases of recolonisation generally proceed very rapidly (1-2 weeks) after a

539 severe devastation (review by Coull and Palmer, 1984; Schratzberger et al., 2004). The rapid dispersal

540 of meiofauna has been ascribed primarily to water column processes, including passive erosion or active

541 emergence (Armonies, 1994, 1988; Palmer et al., 1988; Palmer and Gusf, 1985), but the colonisation of

542 defaunated sediments via lateral interstitial migration has also been observed (Schratzberger et al.,

543 2004).

544

545 ### 3.6. Linking meiofaunal composition and sediment properties

546 Canonical correspondence analysis (CCA) allows to relate the abundance of species to

547 environmental variables (ter Braak, 1986). The canonical ordination diagram summarised the ecological

548 preferences of the meiofaunal taxa at the MESURHO station (Fig. 7). This constrained ordination

549 explained 54% of the total inertia. Permutation tests confirmed that relations between taxa abundances

550 and sediment properties were statistically significant ($p<0.01$) for the sum of all canonical axes (F ratio

551 = 2.3) and for the two first axes (F ratio = 14.9 and 4.2 for axis 1 and axis 2, respectively). Together, the

552 first and second principal canonical axes accounted for 85% of the relationship between taxa and

553 environmental parameters.

554
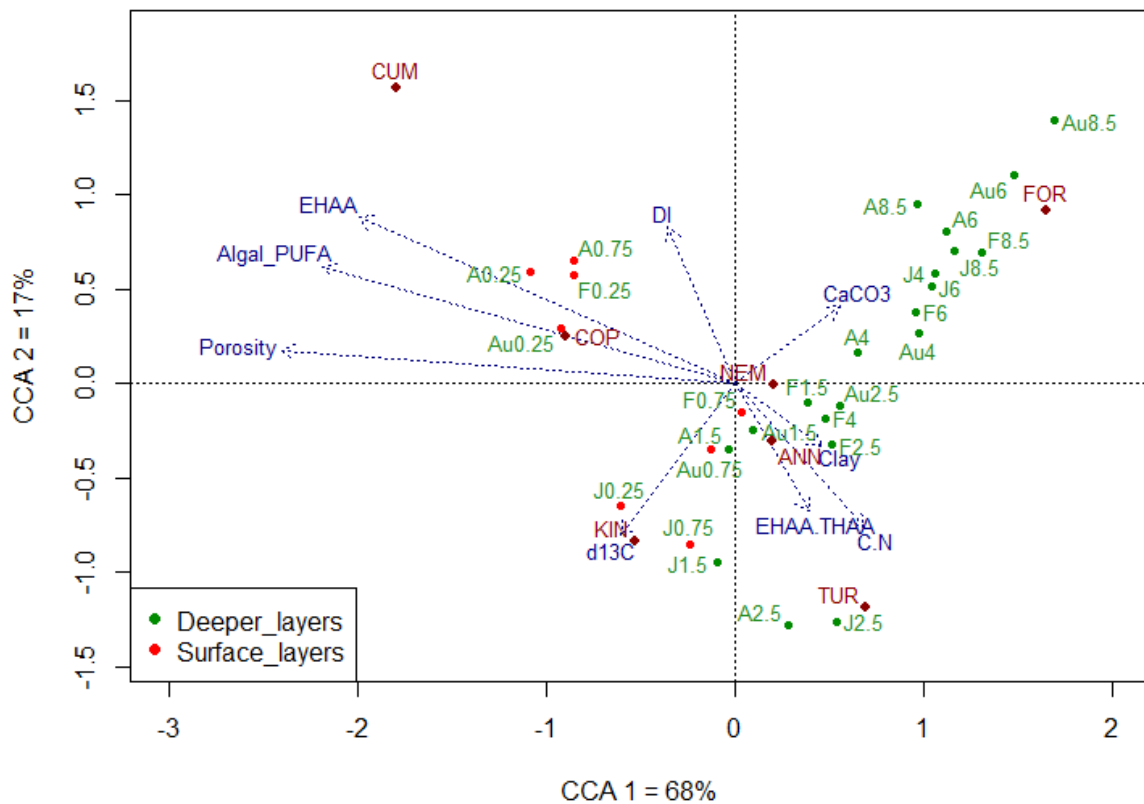
Figure 7: Canonical correspondence analysis (CCA) triplot showing ordination of meiofaunal taxa at the MESURHO site in February, April, July and August 2010 with environmental variables as arrows and samples as dots.

Nematodes (NEM), copepods (COP), kinorhynchs (KIN), annelids (ANN), turbellarians (TUR), cumaceans (CUM), and foraminiferans (FOR). Environmental variables are C/N = molecular carbon to nitrogen ratio, $\delta^{13}C$ = bulk stable isotope value, EHAA: normalised concentration in enzymatically hydrolysable amino acids, EHAA/THAA: enzymatically hydrolysable amino acids to total hydrolysable amino acid ratio, DI= degradation index, algal PUFA = normalised concentration in algal polyunsaturated fatty acids, clay= proportion of clay, $CaCO_3$ = calcium carbonate percentage, and porosity.

Sample code is as follow: the letter indicates the month (F= February, A= April, J= July, Au= August) and the number corresponds to the mid-depth of the sediment layer (in cm). Red dots indicate surface sediment layers (0-0.5cm and 0.5-1cm), and green dots deeper sediment layers (1-2cm, 2-3cm, 3-5cm, 5-7cm, and 7-10cm).

568

569   Among all the candidate environmental constraints, permutation tests showed that porosity,

570   percentage of algal PUFA and normalised concentration of EHAA were the most influential on the

571   meiofauna (Table 3). These three variables were strongly negatively correlated to the first axis, meaning

572   that the main ecological gradient was linked to higher porosity and inputs of labile OM. DI was positively

573   correlated to the second axis, whereas δ^{13}C, C/N and EHAA/THAA were negatively correlated. With no

574   surprise the meiofaunal community was mainly distributed along the first axis according to sediment

575   depth, with negative scores for the surface layers (0-0.5 & 0.5-1 cm) and positive scores for deeper

576   sediments (below 1cm). The meiofauna inhabiting the surface sediments further aggregated on the

577   second axis according to the origin of the OM. As seen before, in February, April and August, fresh

578   suspended particulate matter settled on the seafloor (Fig. 3). The meiofaunal community clearly

579   responded to these inputs of food with higher frequencies of copepods and cumaceans (Fig. 7). A

580   distinct community was found in July in the three first centimetres of the flood deposit. This community

581   was related to higher δ^{13}C, EHAA/THAA, and C/N ratios. Finally, communities from the deepest sediment

582   layers (5-7 and 7-10cm) were grouped and were not related to any of the environmental factors

583   examined in the present study.

584   The constrained ordination also displayed how the meiofaunal taxa were structured with

585   respect to their environmental constraints and agreed well with the known ecological niches of the

586   recorded taxa. Many cumaceans and harpacticoid copepods rely on planktonic diatoms sinking on the

587   seafloor (De Troch et al., 2005; Giere, 2009; Higgins and Thiel, 1988). In good consistency with their

588   feeding habits, cumaceans and copepods were related to inputs of fatty acids produced by

589   phytoplankton and higher level of bioavailable amino acids found on the top of the cores. Kinorhynchs

590   belong to another group with a known preference for the upper (0-3 cm) oxygenated surface layers

591   (Giere, 2009). Shallow water forms feed mainly on diatoms, but they are also linked to organically

592   enriched sediments (Higgins and Thiel, 1988) as those found near river mouths (Guidi-Guilvard and

593   Buscail, 1995). As expected, kinorhynchs were found in the surface sediments, but they displayed high

594   relative frequencies (~13%) in the flood deposit that recovered the seafloor in July. While kinorhynch

595 density in the top layers remained constant from April to August, copepod and cumacean densities

596 dropped remarkably after the flood (Supplementary material, Table S2). This shows that crustaceans

597 and kinorhynchs respond differently to river regime. In a mesocosm study, Rudnick (1989) found that

598 copepods and kinorhynchs belong to two distinct feeding groups; the first group consuming fresh OM,

599 while the second one could use older detrital matter. However, since the sampling only occurred a few

600 days after the flood, it seems unlikely that the nature of the available OM could be the factor affecting

601 meiofaunal community in July. Kinorhynchs can perform vertical movements in the sediment

602 (Shimanaga et al., 2000). A higher capacity to migrate upward and colonise the newly flood deposit

603 could explain the apparent resilience of kinorhynchs to the physical perturbation induced by the high-

604 discharge event. Nematodes and annelids were the taxa whose occurrence and variability in density

605 were the less explained by the CCA. Free-living nematodes, the metazoans with the greatest species

606 richness in the sediments, occupy various ecological niches with different trophic requirements and

607 sediment preferences (Giere, 2009; Moens et al., 2013), which may explain their wide vertical

608 distribution. The ordination showed anyway their preference for subsurface and deeper sediment

609 layers. Like nematodes, meiobenthic annelids are euryoecious, their preferences relate to sediment

610 structure and organic content (Giere, 2009; Villora-Moreno, 1997). In the present study, they were

611 related to ascending EHAA/THAA and C/N ratios. Foraminiferans were associated with deeper sediment

612 layers and $CaCO_3$. Most foraminiferans are versatile for microhabitat selection, food supply and oxygen

613 availability. Mojtahid et al. (2010) investigated microhabitat preferences of living foraminiferans in front

614 of the Rhône River mouth. They found two different assemblages: infaunal species with maximum

615 densities in anoxic layers were dominant close to the river mouth, while species living predominantly in

616 the top surface layer dominated in areas less influenced by fluvial inputs. They postulated that the

617 higher tolerance of infaunal species for degraded terrestrial OM explains their dominance in the

618 prodelta area. This is consistent with the CCA ordination showing that foraminiferans were related to

619 rather low $\delta^{13}C$ (meaning higher contribution of terrestrial OM). Finally, turbellarians, a group with

620 predatory habits or feeding on diatoms, only occurred in two samples (layers 2-3 cm in April and July).

621   Hence, little can be said of their ecological optimum. However, their occurrence is generally determined

622   by the sediment water and oxygen contents (Giere, 2009).

623   The CCA highlighted that the main ecological gradients for the meiofaunal community in the

624   Rhône prodelta were related to sediment depth and river regime. Strong vertical patterns are found in

625   recent sediments with the degradation of the most labile organic components and short-scale variations

626   of abiotic parameters (oxygenation, redox potential…). These vertical patterns constrain the distribution

627   of the meiofauna (Maria et al., 2012). In contrast, river regime accounts for temporal changes in the

628   amount, provenance and nature of the OM accumulated in the prodelta (Cathalot et al., 2010). The

629   relationships between the meiofauna and the biochemical characteristics of sedimentary OM have been

630   previously investigated by de Bovée et al. (1990) and Grémare et al. (2002) in the Gulf of Lion. They

631   reported that meiofaunal abundance correlated better with concentrations in lipids and EHAA rather

632   than with bulk properties of the OM (nitrogen and organic carbon contents) on the shelf ($0 - 175$ m

633   depth range). In the present study, porosity, algal PUFA and EHAA were the best predictors of

634   meiofaunal composition, whereas porosity, $\delta^{13}C$ and DI was the best combination of explanatory

635   variables (Table 3). The strong influence of porosity on the meiofauna is certainly indirect. This factor is

636   related to sediment depth as many other environmental variables not measured in the present study.

637   In particular, porosity partially controls important abiotic factors such as dissolved oxygen diffusion and

638   thus redox potential (Eh). The present results furthermore show that qualitative descriptors of

639   sedimentary organics not only explain spatiotemporal changes in meiofaunal composition (de Bovée et

640   al., 1990; Grémare et al., 2002), but also temporal changes in the vertical distribution of meiofaunal

641   taxa.

642

643   4. Conclusions

644   Major variations of the origin and quality of sedimentary OM are observed in the Rhône River

645   prodelta at a monthly time scale. These fluctuations are mainly controlled by the fast dynamic of the

646   processes affecting river flow and inputs from the watershed, but also by biological and physical

647   processes in the coastal area. Terrestrial organic inputs exported mostly during periods of high river

648   discharge are preserved in the sediments until further remobilisation (Fig. 8). High-discharge events in

649   autumn and winter mostly bring a material enriched in plant detritus, while other events as the one

650   triggered by intense rainfalls in June 2010 are responsible for the transport of more degraded and poorly

651   reactive POC. These different pools of OM (soil, litter, phytodetritus), with variable composition and

652   quality, constitute a variety of trophic resources for the infauna. In this very complex and dynamic

653   system, the meiofaunal community is driven by both trophic conditions and deposition of new sediment

654   layers linked to the hydrological regime of the Rhône River. Inputs of high quality OM (highlighted by

655   fatty acid biomarkers and amino acid indices) appear as a key structuring factor for the meiofauna as

656   already showed by Vanreusel et al. (1995) and Giere (2009). Meiofauna is more abundant in spring when

657   the sedimentation of labile OM originating from the phytoplankton bloom induced eutrophic

658   conditions, whereas meiofaunal densities are low in late summer due to reduced inputs of labile POC

659   (Fig. 8). The current results also point out the rapid response of the meiofauna to a short high-discharge

660   event and the higher importance of analysing the vertical distribution of meiofaunal taxa rather than

661   the total meiofauna abundances, since it was more relevant to show the perturbation. The meiofauna

662   was severely impacted by this physical disturbance with a significant decrease of its total density and

663   the burial of the meiobenthic community under the flood deposit, even though the newly settled layer

664   was rapidly colonised (less than 2 months). The fast recovery of the meiobenthic community highlights

665   that the meiofauna accounts for a highly resilient component of the benthic ecosystem in the vicinity of

666   the Rhône River mouth, in contrast to the macrofauna, which is much longer affected by high-discharge

667   events (Bonifácio et al., 2014).

668
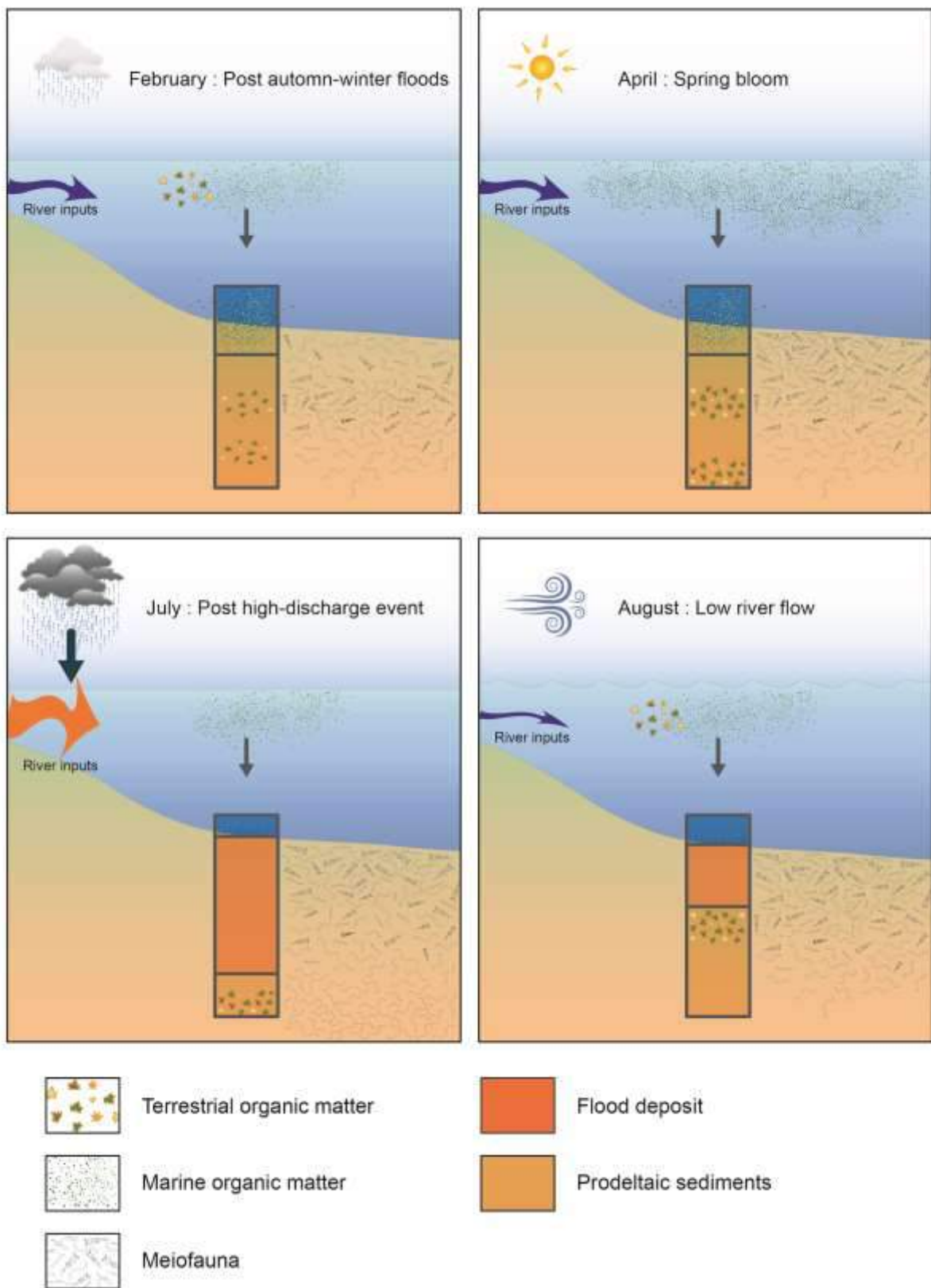
Figure 8: Synthetic scheme of the processes influencing the dynamic of organic matter and meiofaunal community composition during the four investigated periods in the Rhône prodelta.

682   References

683   Akoumianaki, I., Nicolaidou, A., 2007. Spatial variability and dynamics of macrobenthos in a

684   Mediterranean delta front area: The role of physical processes. Journal of Sea Research 57, 47–

685   64. https://doi.org/10.1016/j.seares.2006.07.003

686   Akoumianaki, I., Papaspyrou, S., Kormas, K.Ar., Nicolaidou, A., 2013. Environmental variation and

687   macrofauna response in a coastal area influenced by land runoff. Estuarine, Coastal and Shelf

688   Science, Estuarine and lagoon biodiversity and their natural goods and services 132, 34–44.

689   https://doi.org/10.1016/j.ecss.2012.04.009

690   Akoumianaki, I., Papaspyrou, S., Nicolaidou, A., 2006. Dynamics of macrofaunal body size in a deltaic

691   environment.   Marine   Ecology   Progress   Series   321,   55–66.

692   https://doi.org/10.3354/meps321055

693   Alkhatib, M., Schubert, C.J., del Giorgio, P.A., Gélinas, Y., Lehmann, M.F., 2012. Organic matter reactivity

694   indicators in sediments of the St. Lawrence Estuary. Estuarine, Coastal and Shelf Science 102–

695   103, 36–47. https://doi.org/10.1016/j.ecss.2012.03.002

696   Antonelli, C., Eyrolle, F., Rolland, B., Provansal, M., Sabatier, F., 2008. Suspended sediment and 137Cs

697   fluxes during the exceptional December 2003 flood in the Rhône River, southeast France.

698   Geomorphology 95, 350–360. https://doi.org/10.1016/j.geomorph.2007.06.007

699   Armonies, W., 1994. Drifting meio- and macrobenthic invertebrates on tidal flats in Königshafen: A

700   review. Helgolander Meeresunters 48, 299–320. https://doi.org/10.1007/BF02367043

701   Armonies, W., 1988. Active emergence of meiofauna from intertidal sediment. Marine Ecology Progress

702   Series 43, 151–159. https://doi.org/10.3354/meps043151

703   Balsamo, M., Semprucci, F., Frontalini, F., Coccioni, R., 2012. Meiofauna as a tool for marine ecosystem

704   biomonitoring, in: Marine Ecosystems. In Tech, pp. 77–104. https://doi.org/10.5772/34423

705   Bauer, J.E., Cai, W.-J., Raymond, P.A., Bianchi, T.S., Hopkinson, C.S., Regnier, P.A.G., 2013. The changing

706   carbon cycle of the coastal ocean. Nature 504, 61–70. https://doi.org/10.1038/nature12857

707   Berner, R.A., 1980. Early diagenesis: A theoretical approach. Princeton Univ Pr.

708 Besset, M., Anthony, E.J., Sabatier, F., 2017. River delta shoreline reworking and erosion in the
709   Mediterranean and Black Seas: the potential roles of fluvial sediment starvation and other
710   factors. Elementa: Science of the Anthropocene 5, 54. https://doi.org/10.1525/elementa.139

711 Bianchi, T.S., Allison, M.A., 2009. Large-river delta-front estuaries as natural "recorders" of global
712   environmental change. Proceedings of the National Academy of Sciences 106, 8085–8092.
713   https://doi.org/10.1073/pnas.0812878106

714 Bianchi, T.S., Canuel, E.A., 2011. Chapter 2. Chemical biomarkers applications to ecology and
715   paleoecology, in: Chemical Biomarkers in Aquatic Ecosystems. Princeton University Press, pp.
716   19–29.

717 Blanchet, F.G., Legendre, P., Borcard, D., 2008. Forward selection of explanatory variables. Ecology 89,
718   2623–2632. https://doi.org/10.1890/07-0986.1

719 Bonifácio, P., Bourgeois, S., Labrune, C., Amouroux, J.M., Escoubeyrou, K., Buscail, R., Romero-Ramirez,
720   A., Lantoine, F., Vétion, G., Bichon, S., Desmalades, M., Rivière, B., Deflandre, B., Grémare, A.,
721   2014. Spatiotemporal changes in surface sediment characteristics and benthic macrofauna
722   composition off the Rhône River in relation to its hydrological regime. Estuarine, Coastal and
723   Shelf Science 151, 196–209. https://doi.org/10.1016/j.ecss.2014.10.011

724 Borcard, D., Gillet, F., Legendre, P., 2011. Numerical ecology with R, Use R! Springer, New York.

725 Boudreau, B.P., Jorgensen, B.B., 2001. The Benthic boundary layer: transport processes and
726   biogeochemistry. Oxford University Press.

727 Bourgeois, S., Pruski, A.M., Sun, M.-Y., Buscail, R., Lantoine, F., Kerhervé, P., Vétion, G., Rivière, B.,
728   Charles, F., 2011. Distribution and lability of land-derived organic matter in the surface
729   sediments of the Rhône prodelta and the adjacent shelf (Mediterranean Sea, France): a multi
730   proxy study. Biogeosciences 8, 3107–3125. https://doi.org/10.5194/bg-8-3107-2011

731 Broecker, W., Peng, T., 1974. Gas-Exchange Rates Between Air and Sea. Tellus 26, 21–35.
732   https://doi.org/10.1111/j.2153-3490.1974.tb01948.x

733   Budge, S.M., Parrish, C.C., McKenzie, C.H., 2001. Fatty acid composition of phytoplankton, settling

734   particulate matter and sediments at a sheltered bivalve aquaculture site. Marine Chemistry 76,

735   285–303.

736   Burdige, D.J., Martens, C.S., 1988. Biogeochemical cycling in an organic-rich coastal marine basin: 10.

737   The role of amino acids in sedimentary carbon and nitrogen cycling. Geochimica et

738   Cosmochimica Acta 52, 1571–1584. https://doi.org/10.1016/0016-7037(88)90226-8

739   Cai, W., Reimers, C., 1993. The Development of Ph and Pco2 Microelectrodes for Studying the Carbonate

740   Chemistry of Pore Waters Near the Sediment-Water Interface. Limnol. Oceanogr. 38, 1762–

741   1773. https://doi.org/10.4319/lo.1993.38.8.1762

742   Cardoso, P.G., Raffaelli, D., Lillebø, A.I., Verdelhos, T., Pardal, M.A., 2008. The impact of extreme flooding

743   events and anthropogenic stressors on the macrobenthic communities' dynamics. Estuarine,

744   Coastal and Shelf Science, Submarine groundwater discharge studies along the Ubatuba coastal

745   area in south-eastern Brazil 76, 553–565. https://doi.org/10.1016/j.ecss.2007.07.026

746   Carlier, A., Riera, P., Amouroux, J.-M., Bodiou, J.-Y., Escoubeyrou, K., Desmalades, M., Caparros, J.,

747   Grémare, A., 2007. A seasonal survey of the food web in the Lapalme Lagoon (northwestern

748   Mediterranean) assessed by carbon and nitrogen stable isotope analysis. Estuarine, Coastal and

749   Shelf Science 73, 299–315. https://doi.org/10.1016/j.ecss.2007.01.012

750   Cathalot, C., Rabouille, C., Pastor, L., Deflandre, B., Viollier, E., Buscail, R., Grémare, A., Treignier, C.,

751   Pruski, A., 2010. Temporal variability of carbon recycling in coastal sediments influenced by

752   rivers: assessing the impact of flood inputs in the Rhône River prodelta. Biogeosciences 7, 1187–

753   1205.

754   Cathalot, C., Rabouille, C., Tisnerat-Laborde, N., Toussaint, F., Kerherve, P., Buscail, R., Loftis, K., Sun, M.-

755   Y., Tronczynski, J., Azoury, S., Lansard, B., Treignier, C., Pastor, L., Tesi, T., 2013. The fate of river

756   organic carbon in coastal areas: A study in the Rhone River delta using multiple isotopic (delta

757   C-13, Delta C-14) and organic tracers. Geochimica et Cosmochimica Acta 118, 33–55.

758   https://doi.org/10.1016/j.gca.2013.05.001

759　Copard, Y., Eyrolle, F., Radakovitch, O., Poirel, A., Raimbault, P., Gairoard, S., Di-Giovanni, C., 2018.

760　　　　Badlands as a hot spot of petrogenic contribution to riverine particulate organic carbon to the

761　　　　Gulf of Lion (NW Mediterranean Sea). Earth Surface Processes and Landforms 43, 2495–2509.

762　　　　https://doi.org/10.1002/esp.4409

763　Coull, B.C., 1999. Role of meiofauna in estuarine soft-bottom habitats. Austral Ecology 24, 327–343.

764　　　　https://doi.org/10.1046/j.1442-9993.1999.00979.x

765　Coull, B.C., 1990. Are Members of the Meiofauna Food for Higher Trophic Levels? Transactions of the

766　　　　American Microscopical Society 109, 233–246. https://doi.org/10.2307/3226794

767　Coull, B.C., Chandler, G.T., 1992. Pollution and meiofauna: field, laboratory, and mesocosm studies.

768　　　　Oceanography and Marine Biology: An Annual Review 30, 191–271.

769　Coull, B.C., Palmer, M.A., 1984. Field experimentation in meiofaunal ecology. Hydrobiologia 118, 1–19.

770　　　　https://doi.org/10.1007/BF00031783

771　Danovaro, R., Gambi, C., Manini, E., Fabiano, M., 2000. Meiofauna response to a dynamic river plume

772　　　　front. Marine Biology 137, 359–370. https://doi.org/10.1007/s002270000353

773　Dauwe, B., Middelburg, J.J., Herman, P.M.J., Heip, C.H.R., 1999a. Linking diagenetic alteration of amino

774　　　　acids and bulk organic matter reactivity. Limnology and Oceanography 44, 1809–1814.

775　Dauwe, B., Middelburg, J.J., Van Rijswijk, P., Sinke, J., Herman, P.M.J., Heip, C.H.R., 1999b. Enzymatically

776　　　　hydrolyzable amino acids in North Sea sediments and their possible implication for sediment

777　　　　nutritional values. Journal of Marine Research 57, 109–134.

778　Day, J.W., Ibáñez, C., Pont, D., Scarton, F., 2019a. Chapter 14 - Status and Sustainability of

779　　　　Mediterranean Deltas: The Case of the Ebro, Rhône, and Po Deltas and Venice Lagoon, in:

780　　　　Wolanski, E., Day, J.W., Elliott, M., Ramachandran, R. (Eds.), Coasts and Estuaries. Elsevier, pp.

781　　　　237–249. https://doi.org/10.1016/B978-0-12-814003-1.00014-9

782　Day, J.W., Ramachandran, R., Giosan, L., Syvitski, J., Paul Kemp, G., 2019b. Chapter 9 - Delta Winners

783　　　　and Losers in the Anthropocene, in: Wolanski, E., Day, J.W., Elliott, M., Ramachandran, R. (Eds.),

784   Coasts and Estuaries. Elsevier, pp. 149–165. https://doi.org/10.1016/B978-0-12-814003-

785   1.00009-5

786 de Bovée, F., Guidi, L.D., Soyer, J., 1990. Quantitative distribution of deep-sea meiobenthos in the

787   northwestern Mediterranean (Gulf of Lions). Continental Shelf Research 10, 1123–1145.

788   https://doi.org/10.1016/0278-4343(90)90077-Y

789 De Troch, M., Steinarsdottir, M., Chepurnov, V., Olafsson, E., 2005. Grazing on diatoms by harpacticoid

790   copepods: species-specific density-dependent uptake and microbial gardening. Aquatic

791   Microbial Ecology 39, 135–144.

792 Dufois, F., Verney, R., Le Hir, P., Dumas, F., Charmasson, S., 2014. Impact of winter storms on sediment

793   erosion in the Rhone River prodelta and fate of sediment in the Gulf of Lions (North Western

794   Mediterranean Sea). Continental Shelf Research 72, 57–72.

795   https://doi.org/10.1016/j.csr.2013.11.004

796 Dunstan, G.A., Volkman, J.K., Barrett, S.M., Leroi, J.M., Jeffrey, S.W., 1994. Essential polyunsaturated

797   fatty acids from 14 species of diatom (Bacillariophyceae). Phytochemistry 35, 155–161.

798 Fagervold, S.K., Bourgeois, S., Pruski, A.M., Charles, F., Kerhervé, P., Vetion, G., Galand, P.E., 2014. River

799   organic matter shapes microbial communities in the sediment of the Rhône prodelta. The ISME

800   journal. https://doi.org/10.1038/ismej.2014.86

801 Fontanier, C., Jorissen, F., Lansard, B., Mouret, A., Buscail, R., Schmidt, S., Kerherve, P., Buron, F.,

802   Zaragosi, S., Hunault, G., Ernoult, E., Artero, C., Anschutz, P., Rabouille, C., 2008. Live

803   foraminifera from the open slope between Grand Rhone and Petit Rhone Canyons (Gulf of Lions,

804   NW Mediterranean). Deep Sea Research Part I: Oceanographic Research Papers 55, 1532–1553.

805   https://doi.org/10.1016/j.dsr.2008.07.003

806 Franco, M.A., Soetaert, K., Oevelen, D.V., Gansbeke, D.V., Costa, M.J., Vincx, M., Vanaverbeke, J., 2008.

807   Density, vertical distribution and trophic responses of metazoan meiobenthos to phytoplankton

808   deposition in contrasting sediment types. Marine Ecology Progress Series 358, 51–62.

809   https://doi.org/10.3354/meps07361

810   Franzo, A., Asioli, A., Roscioli, C., Patrolecco, L., Bazzaro, M., Del Negro, P., Cibic, T., 2019. Influence of
811   natural and anthropogenic disturbances on foraminifera and free-living nematodes in four
812   lagoons of the Po delta system. Estuarine, Coastal and Shelf Science 220, 99–110.
813   https://doi.org/10.1016/j.ecss.2019.02.039

814   Gambi, C., Totti, C., Manini, E., 2003. Impact of Organic Loads and Environmental Gradients on
815   Microphytobenthos and Meiofaunal Distribution in a Coastal Lagoon. Chemistry and Ecology
816   19, 207–223. https://doi.org/10.1080/0275754031000119951

817   Gee, J.M., 1989. An ecological and economic review of meiofauna as food for fish. Zoological Journal of
818   The Linnean Society 96, 243–261. https://doi.org/10.1111/j.1096-3642.1989.tb02259.x

819   Giere, O., 2009. Meiobenthology: The Microscopic Motile Fauna of Aquatic Sediments, 2nd ed. Springer-
820   Verlag, Berlin Heidelberg. https://doi.org/10.1007/978-3-540-68661-3

821   Giosan, L., Syvitski, J., Constantinescu, S., Day, J., 2014. Climate change: Protect the world's deltas.
822   Nature News 516, 31. https://doi.org/10.1038/516031a

823   Goineau, A., Fontanier, C., Jorissen, F., Buscail, R., Kerherve, P., Cathalot, C., Pruski, A.M., Lantoine, F.,
824   Bourgeois, S., Metzger, E., Legrand, E., Rabouille, C., 2012. Temporal variability of live (stained)
825   benthic foraminiferal faunas in a river-dominated shelf - Faunal response to rapid changes of
826   the river influence (Rhone prodelta, NW Mediterranean). Biogeosciences 9, 1367–1388.
827   https://doi.org/10.5194/bg-9-1367-2012

828   Grémare, A., Medernach, L., deBovee, F., Amouroux, J.M., Vetion, G., Albert, P., 2002. Relationships
829   between sedimentary organics and benthic meiofauna on the continental shelf and the upper
830   slope of the Gulf of Lions (NW Mediterranean). Marine Ecology Progress Series 234, 85–94.

831   Guidi-Guilvard, L.D., Buscail, R., 1995. Seasonal survey of metazoan meiofauna and surface sediment
832   organics in a non-tidal turbulent sublittoral prodelta (northwestern Mediterranean).
833   Continental Shelf Research 15, 633–653. https://doi.org/10.1016/0278-4343(94)E0036-L

834   Harmelin-Vivien, M., Dierking, J., Bǎnaru, D., Fontaine, M.F., Arlhac, D., 2010. Seasonal variation in stable

835   C and N isotope ratios of the Rhone River inputs to the Mediterranean Sea (2004–2005).

836   Biogeochemistry 100, 139–150. https://doi.org/10.1007/s10533-010-9411-z

837   Harmelin-Vivien, M., Loizeau, V., Mellon, C., Beker, B., Arlhac, D., Bodiguel, X., Ferraton, F., Hermand,

838   R., Philippon, X., Salen-Picard, C., 2008. Comparison of C and N stable isotope ratios between

839   surface particulate organic matter and microphytoplankton in the Gulf of Lions (NW

840   Mediterranean). Continental Shelf Research 28, 1911–1919.

841   https://doi.org/10.1016/j.csr.2008.03.002

842   Hedges, J.I., Clark, W.A., Quay, P.D., Richey, J.E., Devol, A.H., Santos, U. de M., 1986. Compositions and

843   fluxes of particulate organic material in the Amazon River. Limnology and Oceanography 31,

844   717–738.

845   Hedges, J.I., Oades, J.M., 1997. Comparative organic geochemistries of soils and marine sediments.

846   Organic Geochemistry 27, 319–361. https://doi.org/10.1016/S0146-6380(97)00056-9

847   Heip, C.H.R., Vincx, M., Vranken, G., 1985. The ecology of marine nematodes. Oceanography and Marine

848   Biology: An Annual Review.

849   Hermand, R., Salen-Picard, C., Alliot, E., Degiovanni, C., 2008. Macrofaunal density, biomass and

850   composition of estuarine sediments and their relationship to the river plume of the Rhône River

851   (NW Mediterranean). Estuarine, Coastal and Shelf Science 79, 367–376.

852   Higgins, R.P., Thiel, H., 1988. Introduction to the study of meiofauna, illustrée, révisée, réimprimée. ed.

853   Smithsonian Institution Press, University of Maine.

854   Higueras, M., Kerhervé, P., Sanchez-Vidal, A., Calafat, A., Ludwig, W., Verdoit-Jarraya, M., Heussner, S.,

855   Canals, M., 2014. Biogeochemical characterization of the riverine particulate organic matter

856   transferred to the NW Mediterranean Sea. Biogeosciences 11, 157–172.

857   https://doi.org/10.5194/bg-11-157-2014

858 Husson, F., Josse, J., Pages, J., 2010. Principal component methods-hierarchical clustering-partitional

859   clustering: why would we need to choose for visualizing data? Applied Mathematics

860   Department.

861 Jennerjahn, T.C., Ittekkot, V., 1997. Organic matter in sediments in the mangrove areas and adjacent

862   continental margins of Brazil: I. Amino acids and hexosamines. Oceanologica Acta 20, 359–369.

863 Lansard, B., Rabouille, C., Denis, L., Grenz, C., 2008. In situ oxygen uptake rates by coastal sediments

864   under the influence of the Rhone River (NW Mediterranean Sea). Continental Shelf Research

865   28, 1501–1510. https://doi.org/10.1016/j.csr.2007.10.010

866 Lê, S., Josse, J., Husson, F., 2008. FactoMineR: An R Package for Multivariate Analysis | Lê | Journal of

867   Statistical Software 25, 1–18. https://doi.org/10.18637/jss.v025.i01

868 Leithold, E.L., Hope, R.S., 1999. Deposition and modification of a flood layer on the northern California

869   shelf: lessons from and about the fate of terrestrial particulate organic carbon. Marine Geology

870   154, 183–195.

871 Li, Y., Gregory, S., 1974. Diffusion of Ions in Sea-Water and in Deep-Sea Sediments. Geochimica et

872   Cosmochimica Acta 38, 703–714.

873 Lindroth, P., Mopper, K., 1979. High performance liquid chromatographic determination of subpicomole

874   amounts of amino acids by precolumn fluorescence derivatization with ortho-phthaldialdehyde.

875   Analytical Chemistry 51, 1667–1674.

876 Lohrer, A.M., Thrush, S.F., Hewitt, J.E., Berkenbusch, K., Ahrens, M., Cummings, V.J., 2004. Terrestrially

877   derived sediment: response of marine macrobenthic communities to thin terrigenous deposits.

878   Marine Ecology Progress Series 273, 121–138. https://doi.org/10.3354/meps273121

879 Lorthiois, T., 2012. Dynamique des matières en suspension dans le panache du Rhône (Méditerranée

880   occidentale) par télédétection spatiale "couleur de l'océan" (thesis). Université Paris 6.

881 Maillet, G.M., Vella, C., Berné, S., Friend, P.L., Amos, C.L., Fleury, T.J., Normand, A., 2006. Morphological

882   changes and sedimentary processes induced by the December 2003 flood event at the present

883   mouth of the Grand Rhône River (southern France). Marine Geology 234, 159–177.

884 Maria, T.F., Vanaverbeke, J., Esteves, A.M., De Troch, M., Vanreusel, A., 2012. The importance of

885   biological interactions for the vertical distribution of nematodes in a temperate ultra-dissipative

886   sandy beach. Estuarine, Coastal and Shelf Science 97, 114–126. https://doi.org/10.1016/j.ecss.2011.11.030

887   https://doi.org/10.1016/j.ecss.2011.11.030

888 Marion, C., Maillet, G., Arnaud, M., Eyrolle, F., 2010. Quantifications des flux solides rhôdaniens à

889   l'embouchure: apports de la Durance pendant la crue exceptionnelle de mai 2008. La Houille

890   Blanche 72–80. https://doi.org/10.1051/lhb/2010057

891 Martin, D., Pititto, F., Gil, J., Mura, M.P., Bahamon, N., Romano, C., Thorin, S., Schvartz, T., Dutrieux, É.,

892   Bocquenet, Y., 2019. Long-distance influence of the Rhône River plume on the marine benthic

893   ecosystem: Integrating descriptive ecology and predictive modelling. Science of The Total

894   Environment 673, 790–809. https://doi.org/10.1016/j.scitotenv.2019.04.010

895 Mayer, L.M., Schick, L.L., Sawyer, T., Plante, C.J., Jumars, P.A., Self, R.L., 1995. Bioavailable amino acids

896   in sediments: a biomimetic, kinetics-based approach. Limnology and Oceanography 40, 511–

897   520.

898 Meyers, P.A., 1997. Organic geochemical proxies of paleoceanographic, paleolimnologic, and

899   paleoclimatic processes. Organic Geochemistry 27, 213–250.

900 Moens, T., Braeckman, U., Derycke, S., Fonseca, G., Gallucci, F., Ingels, J., Leduc, D., Vanaverbeke, J., Van

901   Colen, C., Vanreusel, A., Vincx, M., 2013. Ecology of free-living marine nematodes, in: Handbook

902   of Zoology: Gastrotricha, Cycloneuralia and Gnathifera, Vol. 2 : Nematoda. De Gruyter, pp. 109–

903   152.

904 Mojtahid, M., Jorissen, F., Lansard, B., Fontanier, C., 2010. Microhabitat selection of benthic

905   foraminifera in sediments off the Rhône River mouth (NW Mediterranean). Journal of

906   Foraminiferal Research 40, 231–246. https://doi.org/10.2113/gsjfr.40.3.231

907 Mojtahid, M., Jorissen, F., Lansard, B., Fontanier, C., Bombled, B., Rabouille, C., 2009. Spatial distribution

908   of live benthic foraminifera in the Rhône prodelta: faunal response to a continental-marine

909   organic matter gradient. Marine Micropaleontology 70, 177–200.

910   https://doi.org/10.1016/j.marmicro.2008.12.006

911   Moloney, C.L., Field, J.G., 1991. The size-based dynamics of plankton food webs. I. A simulation model

912   of carbon and nitrogen flows. Journal of Plankton Research 13, 1003–1038.

913   https://doi.org/10.1093/plankt/13.5.1003

914   Moodley, L., Chen, G., Heip, C.H.R., Vincx, M., Ecosystems Studies, 2000. Vertical distribution of

915   meiofauna in sediments from contrasting sites in the Adriatic Sea: Clues to the role of abiotic

916   versus biotic control. Ophelia 53, 203–212. https://doi.org/10.1080/00785326.2000.10409450

917   Motoda, S., 1959. Devices of simple plankton apparatus. Memoirs of the Faculty of Fisheries, Hokkaido

918   University, 7(1-2), 73-9.

919   Norkko, A., Thrush, S.F., Hewitt, J.E., Cummings, V.J., Norkko, J., Ellis, J.I., Funnell, G.A., Schultz, D.,

920   MacDonald, I., 2002. Smothering of estuarine sandflats by terrigenous clay: the role of wind-

921   wave disturbance and bioturbation in site-dependent macrofaunal recovery. Marine Ecology

922   Progress Series 234, 23–42. https://doi.org/10.3354/meps234023

923   Oksanen, J., Blanchet, F.G., Friendly, M., Kindt, R., Legendre, P., McGlinn, D., Minchin, P.R., O'Hara, R.B.,

924   Simpson, G.L., Solymos, P., Henry, M., Stevens, H., E Szoecs, Wagner, H., 2016. vegan:

925   Community Ecology Package. CRAN: The Comprehensive R Archive Network.

926   O'Leary, J.K., Micheli, F., Airoldi, L., Boch, C., De Leo, G., Elahi, R., Ferretti, F., Graham, N.A.J., Litvin, S.Y.,

927   Low, N.H., Lummis, S., Nickols, K.J., Wong, J., 2017. The Resilience of Marine Ecosystems to

928   Climatic Disturbances. BioScience 67, 208–220. https://doi.org/10.1093/biosci/biw161

929   Olivier, J.-M., Dole-Olivier, M.-J., Amoros, C., Carrel, G., Malard, F., Lamouroux, N., Bravard, J.-P., 2009.

930   Chapter 7 - The Rhône River Basin, in: Tockner, K., Uehlinger, U., Robinson, C.T. (Eds.), Rivers of

931   Europe. Academic Press, London, pp. 247–295. https://doi.org/10.1016/B978-0-12-369449-

932   2.00007-2

933   Palacín, C., Gili, J.-M., Martín, D., 1992. Evidence for coincidence of meiofauna spatial heterogeneity

934   with eutrophication processes in a shallow-water Mediterranean bay. Estuarine, Coastal and

935   Shelf Science 35, 1–16. https://doi.org/10.1016/S0272-7714(05)80053-8

936   Palmer, M.A., Gusf, G., 1985. Dispersal of meiofauna in a turbulent tidal creek. Journal of Marine

937   Research 43, 179–210. https://doi.org/10.1357/002224085788437280

938   Palmer, M.A., Montagna, P.A., Spies, R.B., Hardin, D., 1988. Meiofauna dispersal near natural petroleum

939   seeps in the Santa Barbara channel: A recolonization experiment. Oil and Chemical Pollution 4,

940   179–189.

941   Pastor, L., Deflandre, B., Viollier, E., Cathalot, C., Metzger, E., Rabouille, C., Escoubeyrou, K., Lloret, E.,

942   Pruski, A.M., Vétion, G., Desmalades, M., Buscail, R., Grémare, A., 2011a. Influence of the

943   organic matter composition on benthic oxygen demand in the Rhône River prodelta (NW

944   Mediterranean Sea). Continental Shelf Research 31, 1008–1019.

945   https://doi.org/10.1016/j.csr.2011.03.007

946   Pastor, L., Rabouille, C., Metzger, E., Thibault de Chanvalon, A., Viollier, E., Deflandre, B., 2018. Transient

947   early diagenetic processes in Rhône prodelta sediments revealed in contrasting flood events.

948   Continental Shelf Research 166, 65–76. https://doi.org/10.1016/j.csr.2018.07.005

949   Payrastre, O., Naulin, J.P., Nguyen, C.C., Gaume, E., 2012. Analyse hydrologique des crues de juin 2010

950   dans le Var (Rapport de recherche). IFSTTAR - Institut Français des Sciences et Technologies des

951   Transports, de l'Aménagement et des Réseaux.

952   Pelletier, É., Deflandre, B., Nozais, C., Tita, G., Desrosiers, G., Gagné, J.-P., Mucci, A., 1999. Crue éclair

953   de juillet 1996 dans la région du Saguenay (Québec). 2. Impacts sur les sédiments et le biote de

954   la baie des Ha! Ha! et du fjord du Saguenay. Canadian Journal of Fisheries and Aquatic Sciences.

955   56, 2136–2147. https://doi.org/10.1139/f99-143

956   Pont, D., Simonnet, J.-P., Walter, A.V., 2002. Medium-term Changes in Suspended Sediment Delivery to

957   the Ocean: Consequences of Catchment Heterogeneity and River Management (Rhône River,

958   France). Estuarine, Coastal and Shelf Science 54, 1–18. https://doi.org/10.1006/ecss.2001.0829

959   Pruski, A.M., Buscail, R., Bourgeois, S., Vétion, G., Coston-Guarini, J., Rabouille, C., 2015.

960   Biogeochemistry of fatty acids in a river-dominated Mediterranean ecosystem (Rhône River

961   prodelta, Gulf of Lions, France): Origins and diagenesis. Organic Geochemistry 83–84, 227–240.

962   https://doi.org/10.1016/j.orggeochem.2015.04.002

963   Rabouille, C., 2010a. MESURHOBENT 1 cruise,Téthys II R/V. https://doi.org/10.17600/10450020

964   Rabouille, C., 2010b. MESURHOBENT 2 cruise,Téthys II R/V. https://doi.org/10.17600/10450060

965   Rabouille, C., 2010c. MESURHOBENT 3 cruise,Téthys II R/V. https://doi.org/10.17600/10450100

966   Rabouille, C., 2010d. MESURHOBENT 4 cruise,Téthys II R/V. https://doi.org/10.17600/10450140

967   Rabouille, C., Denis, L., Dedieu, K., Stora, G., Lansard, B., Grenz, C., 2003. Oxygen demand in coastal

968   marine sediments: comparing in situ microelectrodes and laboratory core incubations. Journal

969   of Experimental Marine Biology and Ecology 285–286, 49–69. https://doi.org/10.1016/S0022-

970   0981(02)00519-1

971   Rassmann, J., Eitel, E.M., Lansard, B., Cathalot, C., Brandily, C., Taillefert, M., Rabouille, C., 2020. Benthic

972   alkalinity and dissolved inorganic carbon fluxes in the Rhone River prodelta generated by

973   decoupled aerobic and anaerobic processes. Biogeosciences 17, 13–33.

974   https://doi.org/10.5194/bg-17-13-2020

975   Riera, P., Hubas, C., 2003. Trophic ecology of nematodes from various microhabitats of the Roscoff Aber

976   Bay (France): importance of stranded macroalgae evidenced through $\delta 13C$ and $\delta 15N$. Marine

977   Ecology Progress Series 260, 151–159. https://doi.org/10.3354/meps260151

978   Rudnick, D., 1989. Time lags between the deposition and meiobenthic assimilation of phytodetritus.

979   Marine Ecology Progress Series 50, 231-240. https://doi.org/10.3354/meps050231

980   Salen-Picard, C., Arlhac, D., Alliot, E., 2003. Responses of a Mediterranean soft bottom community to

981   short-term (1993-1996) hydrological changes in the Rhône river. Marine Environmental

982   Research 55, 409–427.

983   Schratzberger, M., Ingels, J., 2018. Meiofauna matters: The roles of meiofauna in benthic ecosystems.

984   Biology and Ecology 502, 125-25.

985   Schratzberger, M., Whomersley, P., Warr, K., Bolam, S.G., Rees, H.L., 2004. Colonisation of various types
986   of sediment by estuarine nematodes via lateral infaunal migration: a laboratory study. Marine
987   Biology 145, 69–78. https://doi.org/10.1007/s00227-004-1302-1

988   Scott, D.B., Tobin, R., Williamson, M., Medioli, F.S., Latimer, J.S., Boothman, W.A., Asioli, A., Haury, V.,
989   2005. Pollution monitoring in two North American estuaries: historical reconstructions using
990   benthic   foraminifera.   Journal   of   Foraminiferal   Research   35,   65–82.
991   https://doi.org/10.2113/35.1.65

992   Semprucci, F., Balsamo, M., Appolloni, L., Sandulli, R., 2018. Assessment of ecological quality status
993   along the Apulian coasts (eastern Mediterranean Sea) based on meiobenthic and nematode
994   assemblages. Mar Biodiv 48, 105–115. https://doi.org/10.1007/s12526-017-0745-9

995   Semprucci, F., Facca, C., Ferrigno, F., Balsamo, M., Sfriso, A., Sandulli, R., 2019. Biotic and abiotic factors
996   affecting seasonal and spatial distribution of meiofauna and macrophytobenthos in transitional
997   coastal   waters.   Estuarine,   Coastal   and   Shelf   Science,   219,   328–340.
998   https://doi.org/10.1016/j.ecss.2019.02.008

999   Shimanaga, M., Kitazato, H., Shirayama, Y., 2000. Seasonal Patterns of Vertical Distribution between
1000   Meiofaunal Groups in Relation to Phytodetritus Deposition in the Bathyal Sagami Bay, Central
1001   Japan. Journal of Oceanography 56, 379–387. https://doi.org/10.1023/A:1011120204419

1002 Soetaert, K., Vincx, M., Wittoeck, J., Tulkens, M., 1995. Meiobenthic distribution and nematode
1003   community   structure   in   five   European   estuaries.   Hydrobiologia   311,   185–206.
1004   https://doi.org/10.1007/BF00008580

1005 ter Braak, C.J.F., 1986. Canonical Correspondence Analysis: A New Eigenvector Technique for
1006   Multivariate   Direct   Gradient   Analysis.   Ecology   67,   1167–1179.
1007   https://doi.org/10.2307/1938672

1008 Tesi, T., Langone, L., Goñi, M.A., Miserocchi, S., Bertasi, F., 2008. Changes in the composition of organic
1009   matter from prodeltaic sediments after a large flood event (Po River, Italy). Geochimica et
1010   Cosmochimica Acta 72, 2100–2114. https://doi.org/10.1016/j.gca.2008.02.005

1011   Ulses, C., Estournel, C., Durrieu de Madron, X., Palanques, A., 2008. Suspended sediment transport in

1012   the Gulf of Lions (NW Mediterranean): Impact of extreme storms and floods. Continental Shelf

1013   Research 28, 2048–2070. https://doi.org/10.1016/j.csr.2008.01.015

1014   Vanaverbeke, J., Steyaert, M., Soetaert, K., Rousseau, V., Van Gansbeke, D., Parent, J.-Y., Vincx, M., 2004.

1015   Changes in structural and functional diversity of nematode communities during a spring

1016   phytoplankton bloom in the southern North Sea. Journal of Sea Research 52, 281–292.

1017   https://doi.org/10.1016/j.seares.2004.02.004

1018   Vanreusel, A., Vincx, M., Schram, D., Gansbeke, D. van, 1995. On the Vertical Distribution of the

1019   Metazoan Meiofauna in Shelf Break and Upper Slope Habitats of the NE Atlantic. Internationale

1020   Revue   der   gesamten   Hydrobiologie   und   Hydrographie   80,   313–326.

1021   https://doi.org/10.1002/iroh.19950800218

1022   Villora-Moreno, S., 1997. Environmental Heterogeneity and the Biodiversity of Interstitial Polychaeta.

1023   Bulletin of Marine Science 60, 494–501.

1024

1025   Table 1: Principal descriptors used in this study with their interpretation.

Descriptors	Feature	Main diagnostic information	References
C/N	Source/Quality	Marine derived OM (6-9), Soil derived OM (8-20) and higher plants (>20); may decrease during OM decomposition	Moloney and Field (1991), Hedges and Oades (1997), Meyers (1997)
$\delta^{13}C$	Source	Marine OM (−20.1±0.8‰) and Rhône River inputs (−27.1 ± 0.6‰)	Harmelin-Vivien et al. (2008) and Higueras et al. (2014)
DI	Quality	Diagenetic alteration of OM with DI values ranging from −2.2 extensively degraded sediments to -1.5 for fresh algae	Dauwe et al. (1999b)
RI	Quality	Selective degradation during diagenesis and production of non-proteic amino acids, lower values in degraded sediments	Jennerjahn & Ittekkot (1997)
EHAA/THAA (%)	Quality	OM bioavailability for the benthic fauna ranging from 0 to 100%	Mayer et al. (1995)
MC-SAFA	Source	Mixed origin, but shorter chains predominate in phytoplankton	Dunstan et al. (1994), Bianchi and Canuel (2011)
LC-SAFA	Source	Terrestrial higher plants, macrodetritus	Bianchi and Canuel (2011), Dunstan et al. (1994), Pruski et al. (2015)
Ter PUFA	Source	Terrestrial higher plants (>2.5%)	Budge et al. (2001), Pruski et al. (2015)
Algal PUFA	Source	Phytoplankton with $C_{20:5\omega3}$ specific of diatoms	Dunstan et al. (1994)
MUFA	Source	Mixed origin with $C_{16:1\omega7}$ common in diatoms and bacteria	Bianchi and Canuel (2011), Dunstan et al. (1994)
BAFA	Source	Bacterial sources	Bianchi and Canuel (2011)

1026   The degradation index (DI), reactivity index (RI) and enzymatically hydrolysable amino acids to total hydrolysable amino acids ratio (EHAA/THAA) are
1027   inferred from the amino acid composition. Fatty acid biomarkers are grouped as follows: mid-chain even-number saturated fatty acids with less than 20
1028   carbons (MC-SAFAs), long-chain saturated fatty acids with 24 carbon or more (LC-SAFA), polyunsaturated fatty acids with 18 carbons ($C_{18:2\omega6}$ and $C_{18:3\omega3}$,
1029   Terr PUFA), the remaining PUFA attributed to microalgae (Algal PUFA), the monounsaturated fatty acids (MUFA) and the straight and branched odd-
1030   numbered fatty acids of bacterial origin (BAFA). The unsaturation index is calculated as the sum of products of the number of double bonds of each acid
1031   multiplied by its percentage of the total fatty acid composition.

1032

1033 Table 2: Temporal variations of Diffusive Oxygen Uptake (DOU) rates in the sediments of the Rhône River

1034 **prodelta in April, July and August 2010.** Values are means ± standard deviations (n= 4), nd= not

1035 determined.

1036

Stations	DOU		
	April 2010	**July 2010**	**August 2010**
MESURHO	16.9 ± 4.1	10.1 ± 0.6	9 ± 1.5
A	14.9 ± 1.3	10.6 ± 3.6	nd
AK	19.7 ± 3.5	11.4 ± 1.3	nd
B	12.7 ± 2.1	11.3 ± 2.9	nd
K	14.9 ± 2.6	11.8 ± 4.9	nd

1037

1038

1039 **Table 3:** Marginal and conditional effects of environmental variables determined using forward selection. Ranking is based on their P-value and Akaike

1040 Information Criterion (AIC) where the variable with the lowest AIC value is the most influential. 999 permutations. Significant variables are indicated in

1041 bold, * p<0.05, ** p<0.01. Best combination of variables: Porosity + δ^{13}C + DI.

1042

1043

Marginal effects						Conditional effects					
Rank	Variable	AIC	F ratio	Pr(>F)		Rank	Variable	AIC	F ratio	Pr(>F)	
1	**Porosity**	79.935	7.267	0.005	**	1	**Porosity**	79.935	7.267	0.005	**
2	**Algal PUFA**	81.865	5.0518	0.005	**	2	**δ^{13}C**	78.509	3.2544	0.015	*
3	**EHAA**	81.042	5.9774	0.015	**	3	**DI**	77.785	2.4517	0.045	*
4	C/N	85.621	1.1536	0.270		-	EHAA	78.170	1.3657	0.180	
5	δ^{13}C	85.715	1.0625	0.385		-	Clay	78.285	1.2658	0.290	
6	EHAA/THAA	86.120	0.6742	0.575		-	Algal PUFA	78.507	1.0746	0.400	
7	DI	86.174	0.6229	0.605		-	EHAA/THAA	79.305	0.3983	0.795	
8	CaCO$_3$	86.252	0.5482	0.655		-	CaCO$_3$	79.301	0.4013	0.820	
9	Clay	86.343	0.4626	0.715		-	C/N	79.419	0.303	0.925	

1044